Localized states in nonlinear topological photonics

Daria Smirnova

Nonlinear Physics Center, Australian National University

Australian National University

Australian Government

Australian Research Council

Acknowledgements

Prof. Yuri Kivshar

Australian National University

Prof. Alexander Khanikaev

The City University of New York

Dr. Daniel Leykam

NUS National University of Singapore

Topological photonics

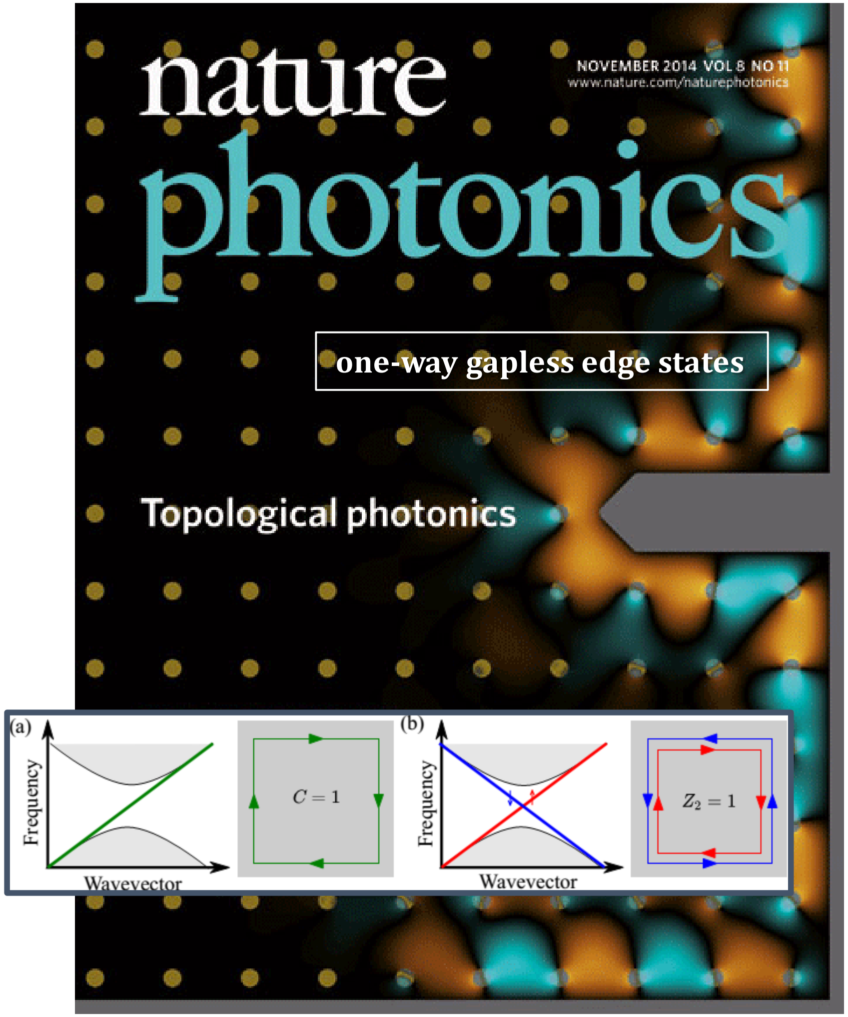

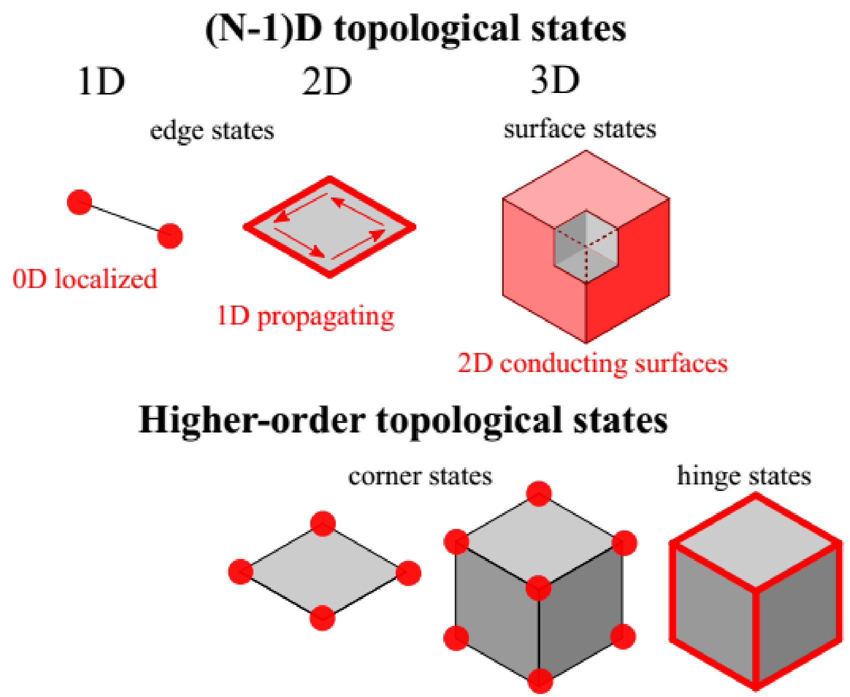

Topological classes
in different dimensions

Lu et al, Nature Photonics **8**, 821 (2014)
Ozawa et al, Rev. Mod. Phys. **91**, 015006 (2019)

Topological Photonics goes Nonlinear

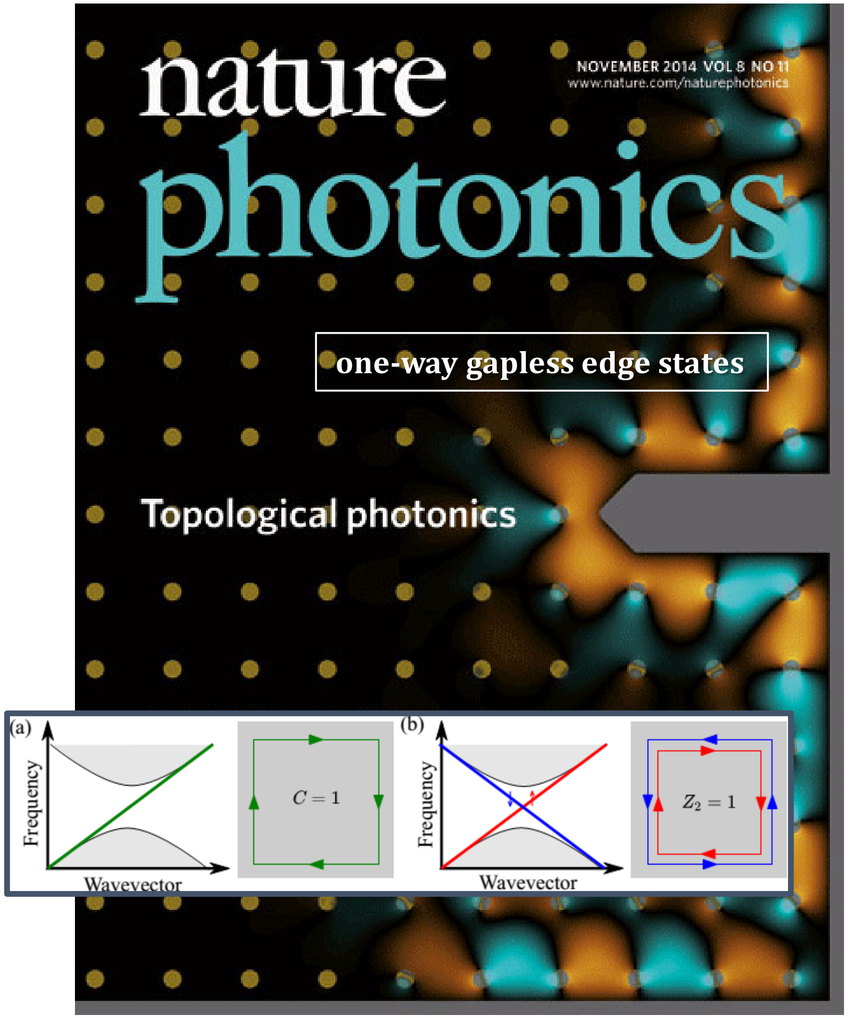

Lu et al, Nature Photonics **8**, 821 (2014)
Ozawa et al, Rev. Mod. Phys. **91**, 015006 (2019)

Applied Physics Reviews

Nonlinear topological photonics

Daria Smirnova,[1] Daniel Leykam,[2,3] Yidong Chong,[4] and Yuri Kivshar[1,a)]

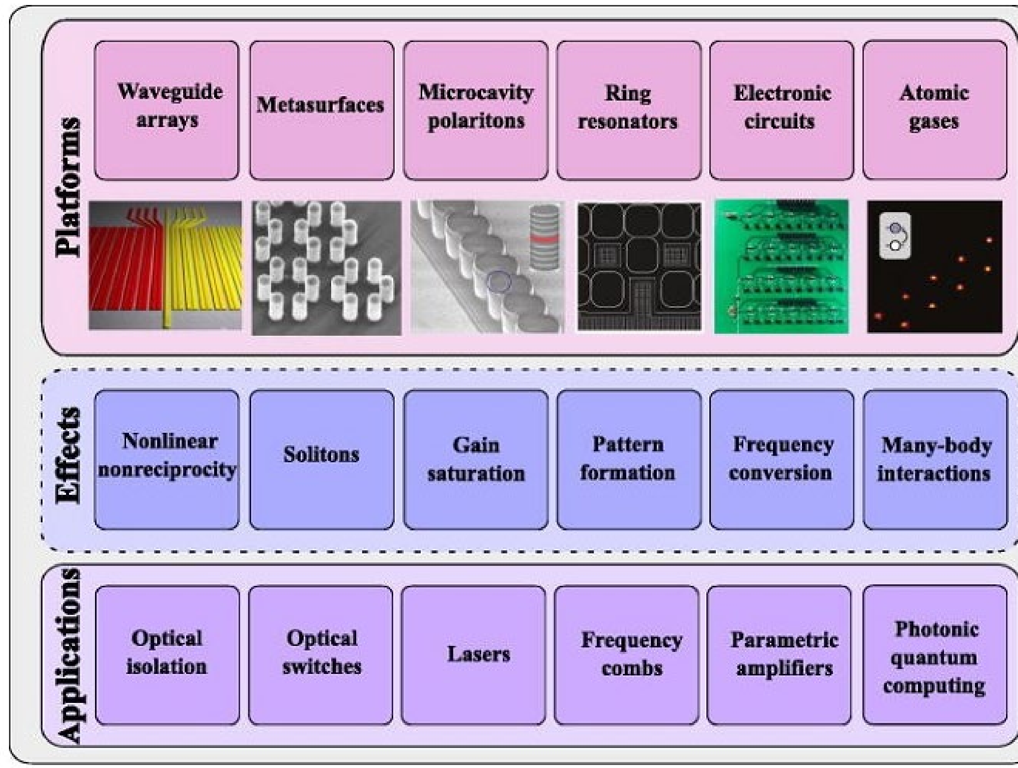

Smirnova et al, Appl. Phys. Rev. **7**, 021306 (2020)

Towards miniaturization

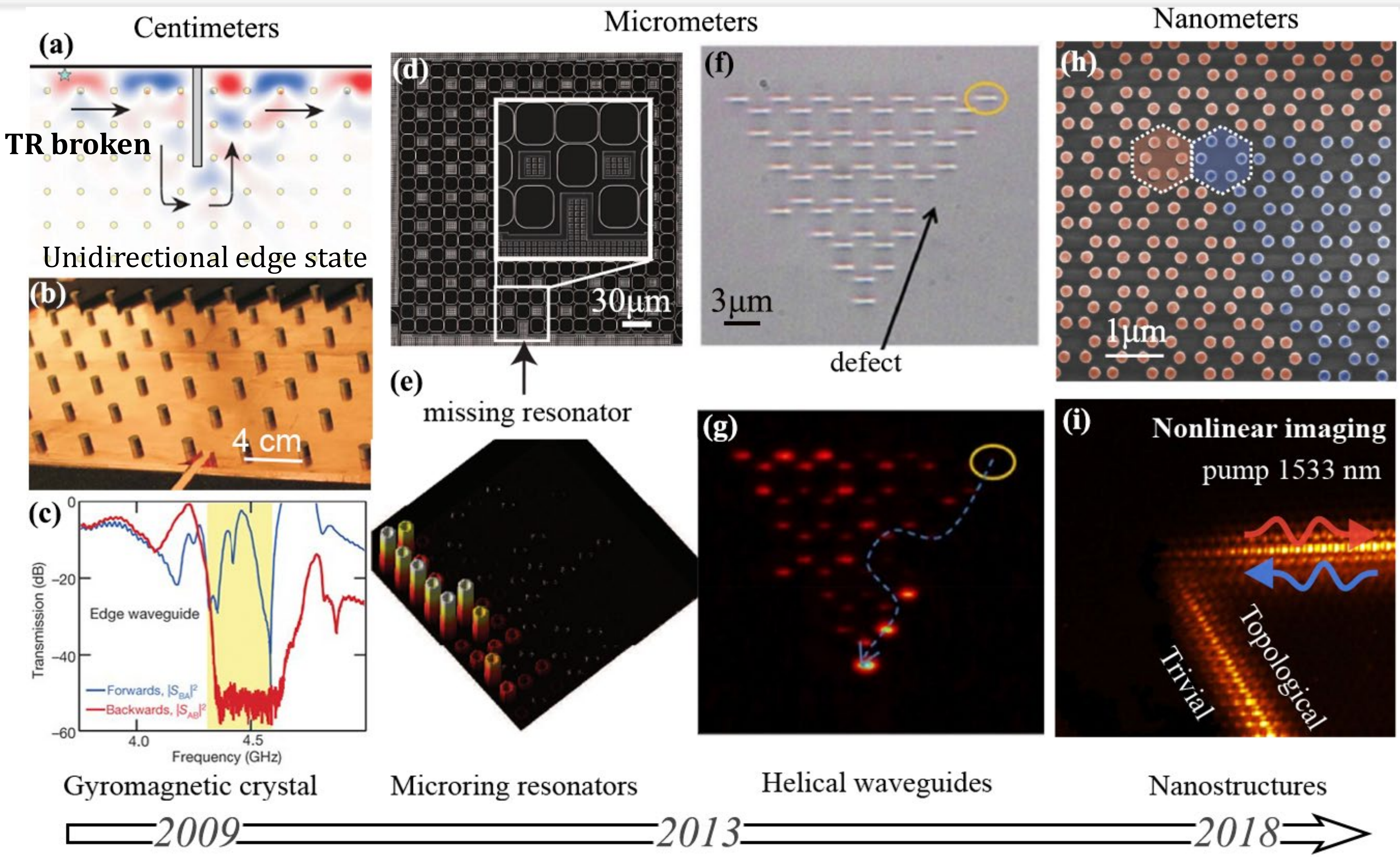

Wang, Chong et al, Nature (2009)

Rechtsman et al, Nature (2013);
Hafezi et al, Nature Photon.(2013)

Barik et al, Science (2018)
Smirnova et al, Phys. Rev. Lett. (2019)

Our scope: All-dielectric platform

TR preserved

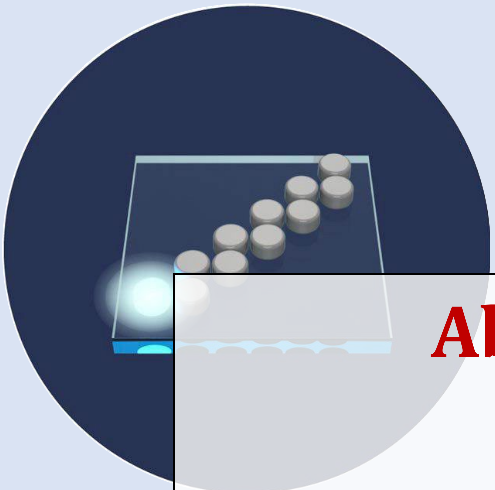

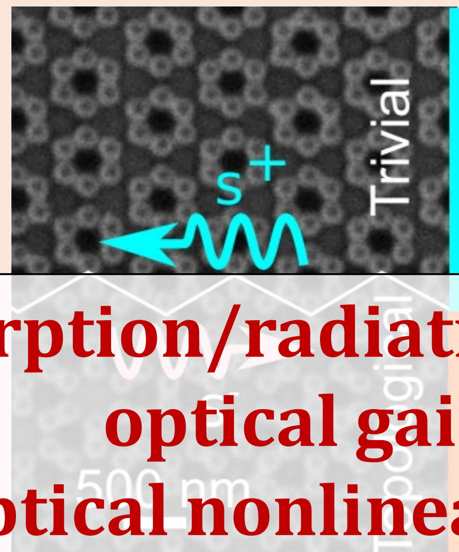

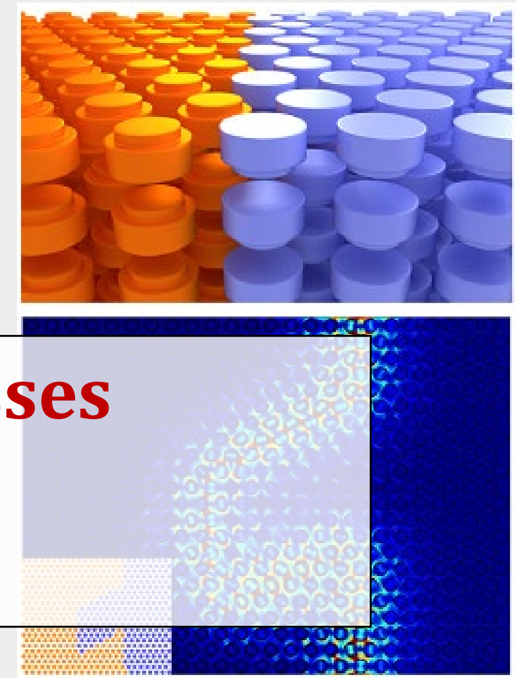

Absorption/radiation losses
optical gain
optical nonlinearities

Zigzag arrays
of resonant particles
1D

Kruk et al, Nature Nanotech. **14**, 126–130 (2018)

Metasurfaces
2D

Gorlach et al, Nat. Comm. **9**, 909 (2018)
Smirnova et al, PRL **123**, 03901 (2019)

Lattice engineering

Metacrystals of bianisotropic particles
2D and 3D

Slobozhanyuk et al, APL **114**, 031103 (2019)
Nature Photonics **11**, 130-136 (2017)

Modification of on-site properties

Nonlinear optics with nanoparticles

Mie resonances

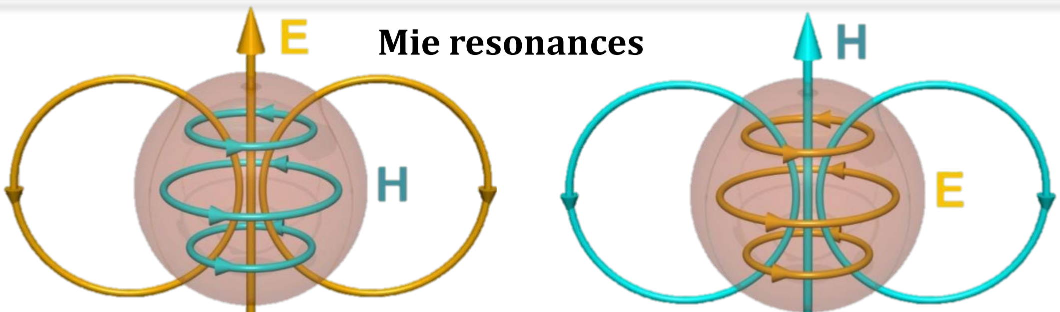

electric dipole mode

magnetic dipole mode

optics and IR

Multipolar decomposition

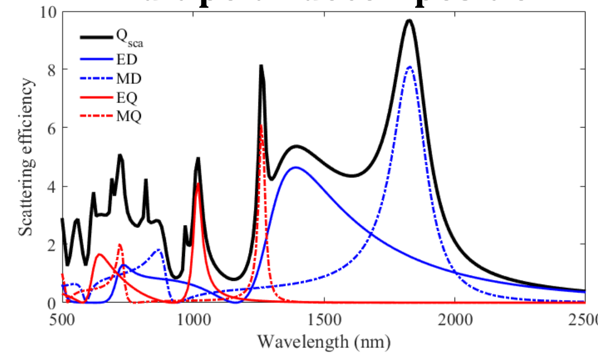

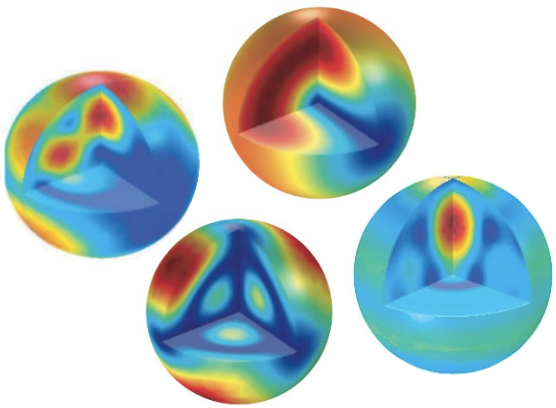

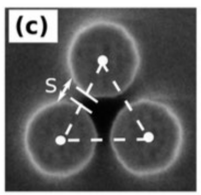

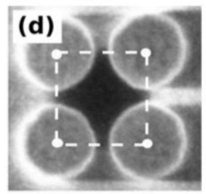

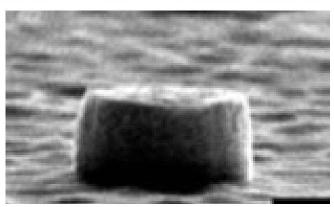

AlGaAs, GaAs, $BaTiO_3$, Si

Review Article
Vol. 3, No. 11 / Optica 1
optica

Multipolar nonlinear nanophotonics

Daria Smirnova and Yuri S. Kivshar*

Frequency conversion by Mie-resonant dielectric nanoparticles

THG

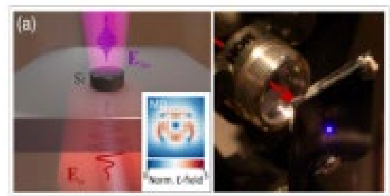

Shcherbakov, Nano Lett. (2014)

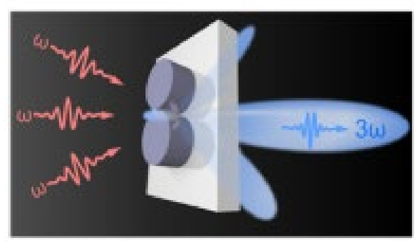

L. Wang, Nanoscale (2017)

SHG

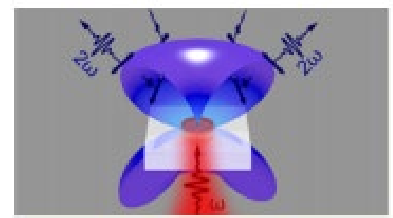

Gili, V. F. Opt. Express (2016)

Liu, S. Nano Lett. (2016)

Camacho-Morales Nano Lett (2016)

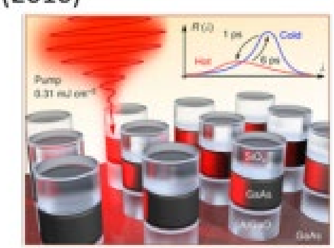

Zigzag array of resonant particles

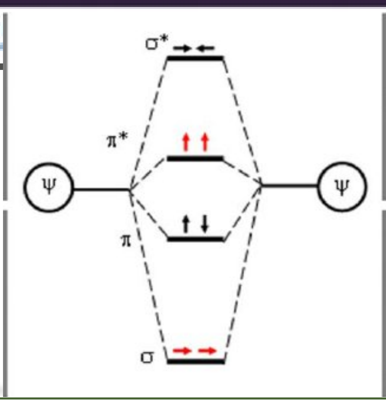

Strong and weak dipole-dipole coupling

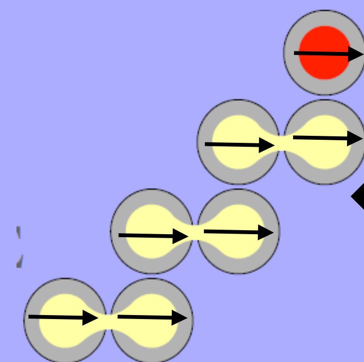

polarization-enriched SSH

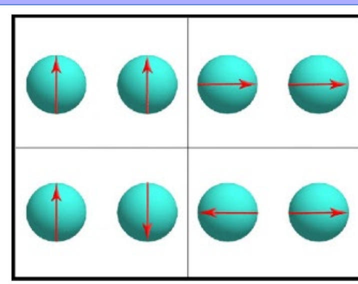

dipole-dipole interactions

Polyacetylene

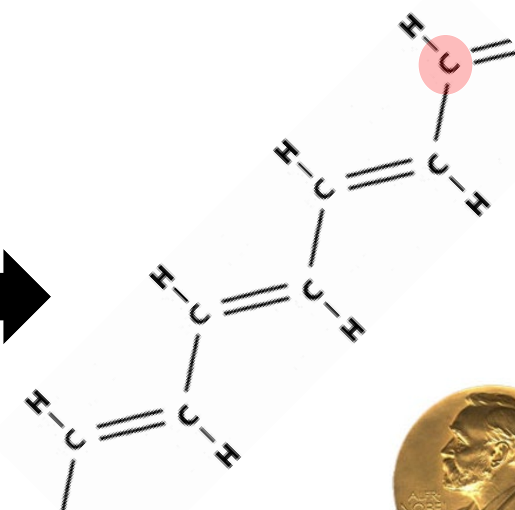

High Electrical Conductivity

Chemistry 2000

Su-Schrieffer-Heeger (SSH) model

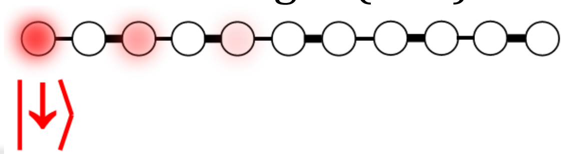

Third-harmonic generation in zigzag arrays

Interplay between ED and MD resonances:

$$\begin{pmatrix} p_{j,x} \\ m_{j,y} \end{pmatrix} - \alpha(\omega)\left[g_{j,j-1}\begin{pmatrix} p_{j-1,x} \\ m_{j-1,y} \end{pmatrix} + g_{j,j+1}\begin{pmatrix} p_{j+1,x} \\ m_{j+1,y} \end{pmatrix} \right] = \alpha(\omega)\begin{pmatrix} E \\ H \end{pmatrix}, \quad \begin{pmatrix} E \\ H \end{pmatrix}_{\pm} = \begin{pmatrix} 1 \\ \pm 1 \end{pmatrix}$$

where the coupling is described by the Green functions

$$g_{2k,2k-1} = g_{2k-1,2k} = t\begin{pmatrix} 2 & 0 \\ 0 & -1 \end{pmatrix}, \quad g_{2k,2k-1} = g_{2k-1,2k} = t\begin{pmatrix} -1 & 0 \\ 0 & 2 \end{pmatrix}$$

and the bianisotropic polarizability tensor is

$$\alpha^{-1}(\omega) = \begin{pmatrix} \frac{\omega_{ED}-\omega-i\Gamma_{ED}}{\Gamma_{0,ED}} & ib \\ -ib & \frac{\omega_{MD}-\omega-i\Gamma_{MD}}{\Gamma_{0,MD}} \end{pmatrix}.$$

Topological phase transition

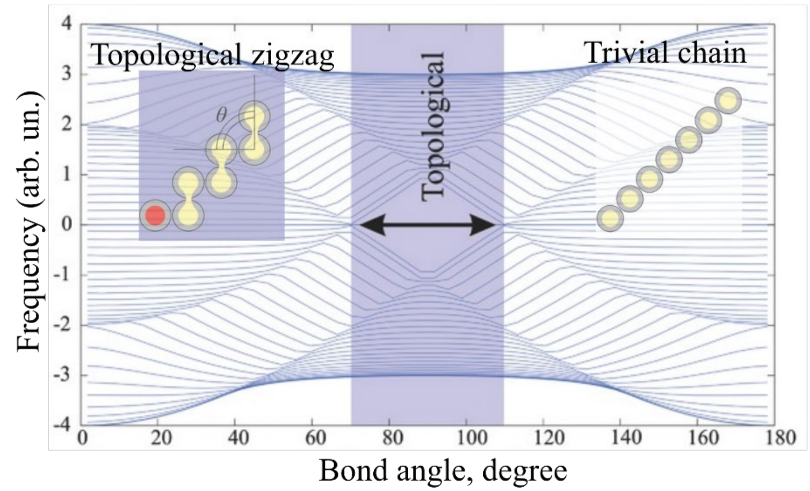

Top/bottom excitation asymmetry

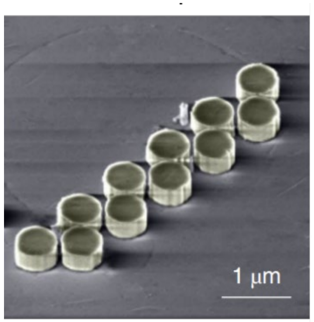

Si nanodisks

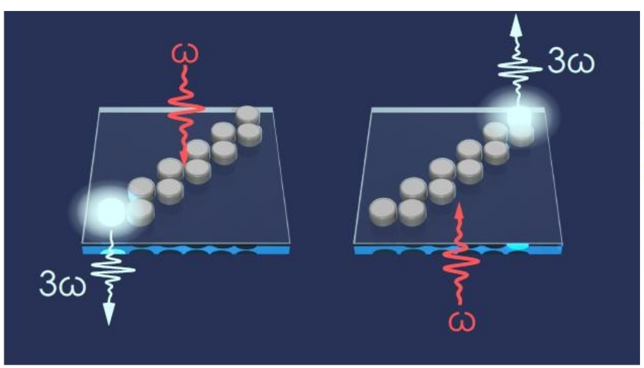

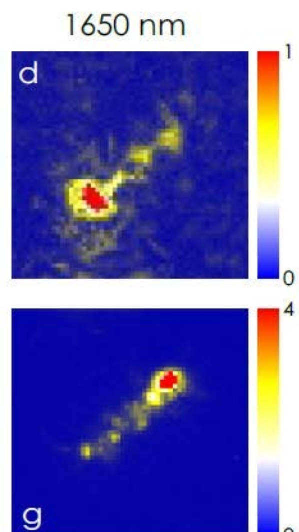

Topological robustness

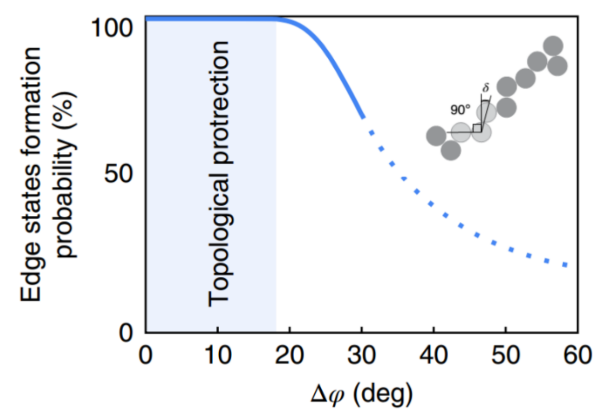

Multipolar decompositions for bianisotropic nanoparticles

Unperturbed disk

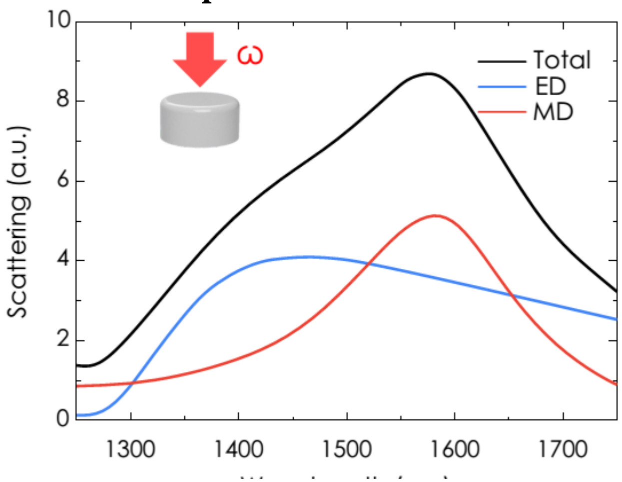

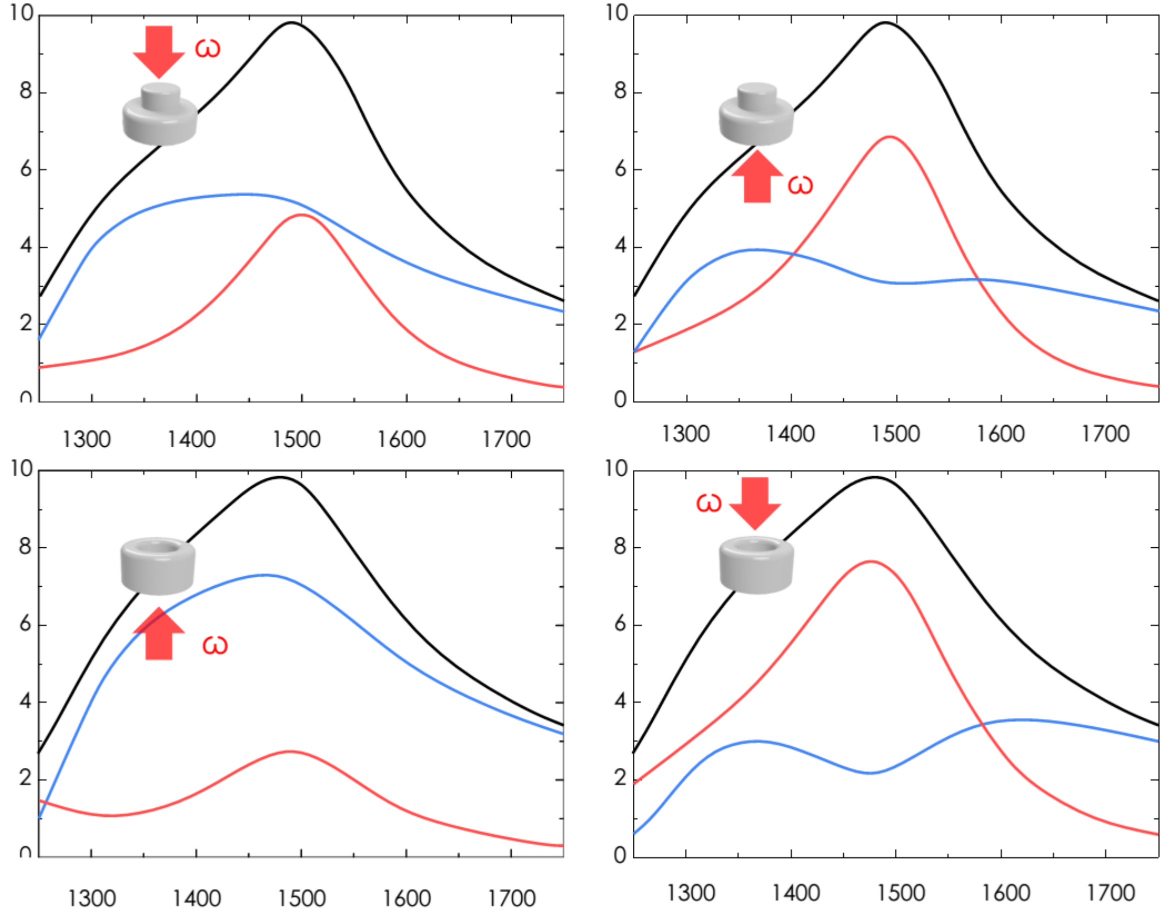

Symmetry reduction

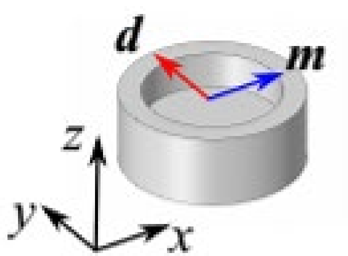

$$\begin{cases} \mathbf{p}_n = \hat{\alpha}^{ee}_n \mathbf{E}_n + \boxed{\hat{\alpha}^{em}_n} \mathbf{H}_n \\ \mathbf{m}_n = \boxed{\hat{\alpha}^{me}_n} \mathbf{E}_n + \hat{\alpha}^{mm}_n \mathbf{H}_n \end{cases}$$

THG is primarily driven by the magnetic dipole excitation.

Topological states mediated by staggered bianisotropy

Staggered-bianisotropy SSH

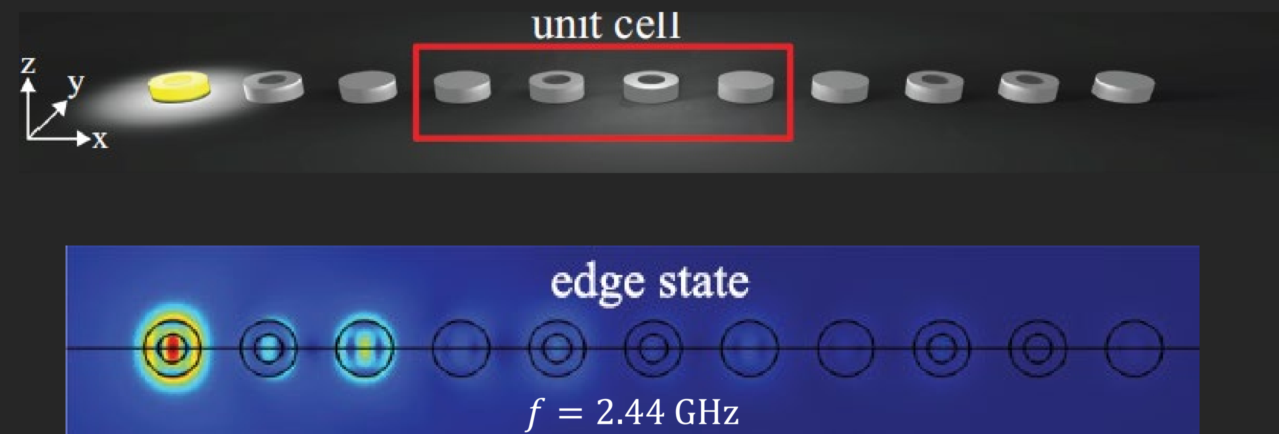

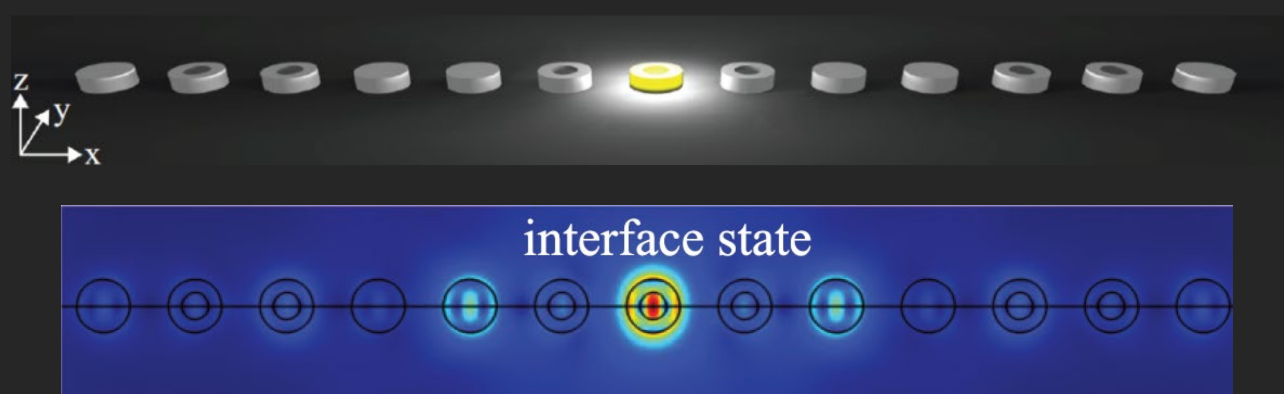

Bobylev, Smirnova, Gorlach, Laser Photonics Rev. **15**, 115110 (2021)

Topological nanophotonic metasurfaces

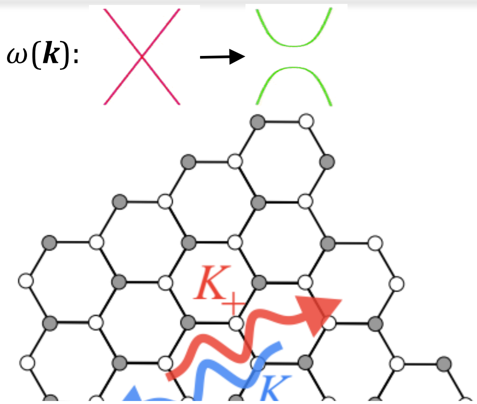

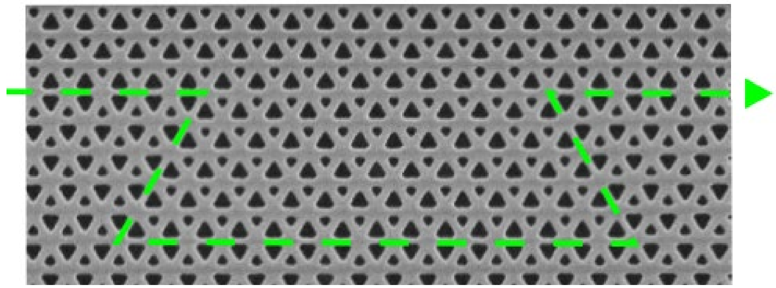

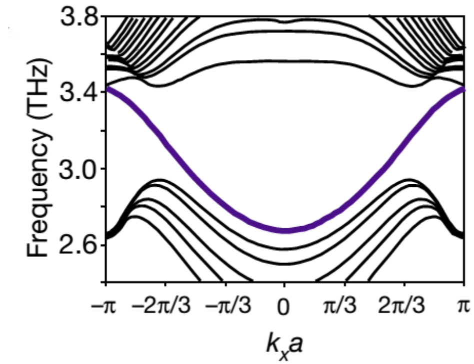

Model	Hamiltonian	Topological invariant
Haldane	$\hat{H} = v_D(\hat{\sigma}_x\hat{\tau}_z\delta k_x + \hat{\sigma}_y\hat{\tau}_0\delta k_y) + \hat{\sigma}_z(\hat{\tau}_z m_T - \hat{\tau}_0 m_I)$	Chern number $C = \frac{1}{2}(\mathrm{sgn}(m_I - m_T) - \mathrm{sgn}(m_I + m_T))$
Kane–Mele	$\hat{H} = v_D\hat{s}_0(\hat{\sigma}_x\hat{\tau}_z\delta k_x + \hat{\sigma}_y\hat{\tau}_0\delta k_y) + \hat{\sigma}_z\hat{\tau}_z\hat{s}_z m_{SO}$	Spin Chern number $C^{spin} = \mathrm{sgn}\,(m_{SO})$
Bernevig–Hughes–Zhang	$\hat{H} = v_D(\hat{\sigma}_x\hat{s}_x\delta k_x + \hat{\sigma}_y\hat{s}_0\delta k_y) + \hat{\sigma}_z\hat{s}_0(m + \beta\delta k^2)$	Spin Chern number $C^{spin} = \frac{1}{2}\,(\mathrm{sgn}\, m - \mathrm{sgn}\,\beta)$
Staggered graphene	$\hat{H} = v_D(\hat{\sigma}_x\hat{\tau}_z\delta k_x + \hat{\sigma}_y\hat{\tau}_0\delta k_y) - \hat{\sigma}_z\hat{\tau}_0 m_I$	Valley Chern number $C^{valley} = \pm\frac{1}{2}\mathrm{sgn}(m_I)$

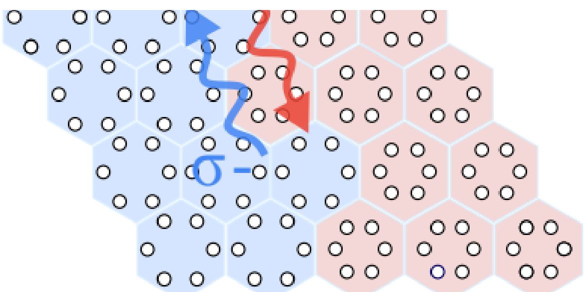

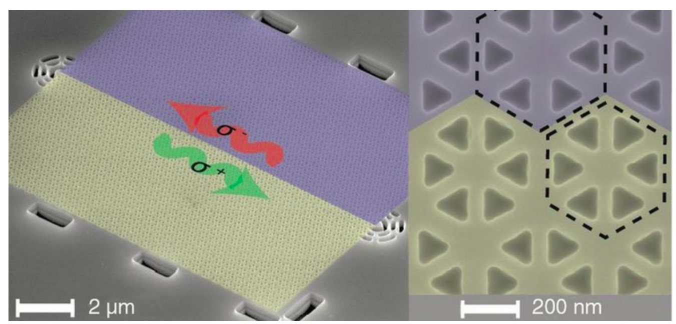

Barik et al, Science (2018)

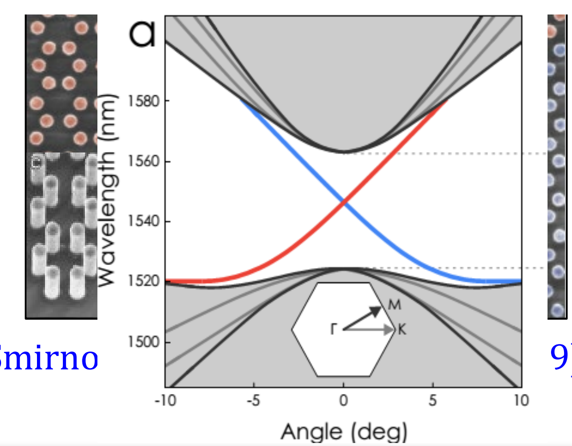

Smirno 9)

Nonlinear imaging of edge states

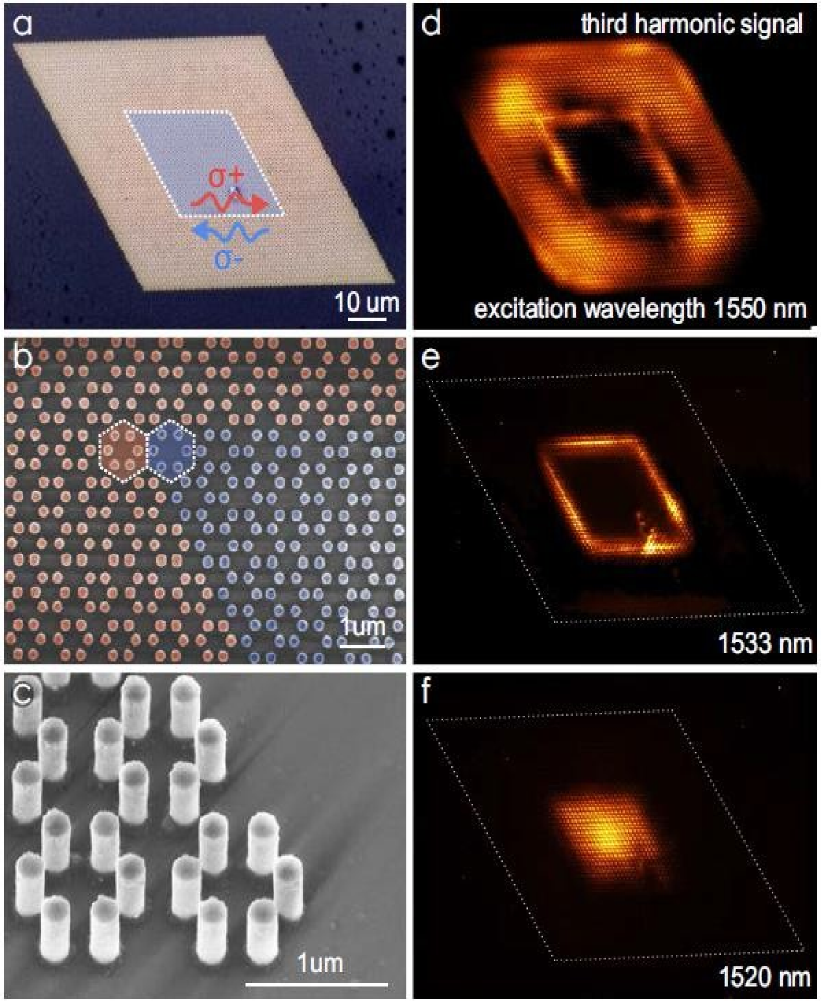

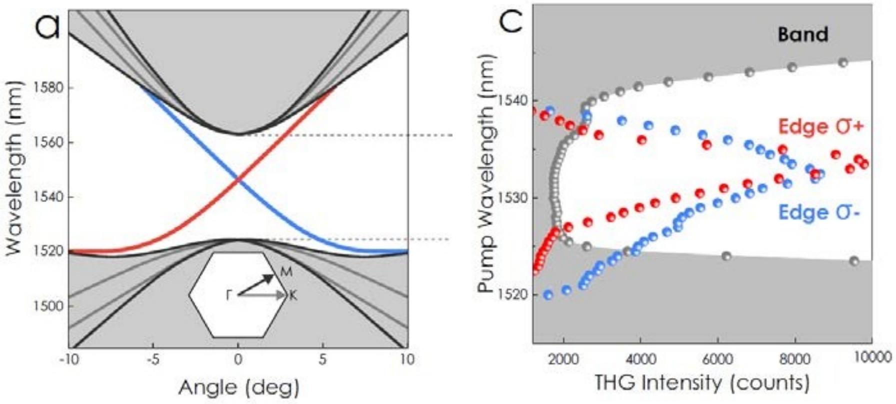

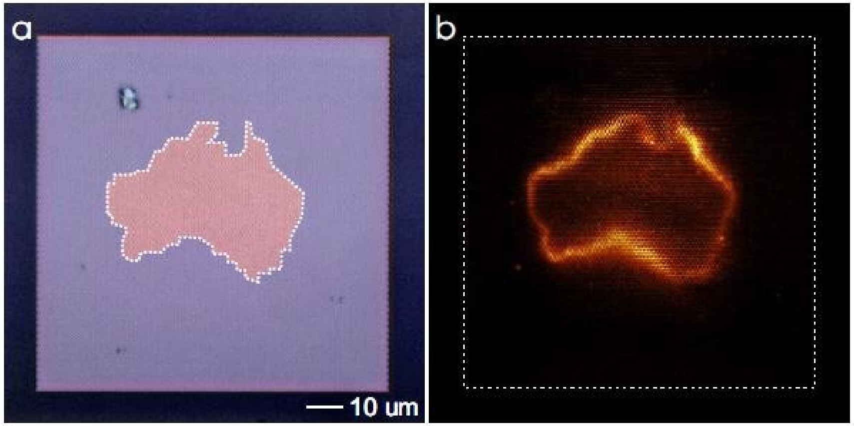

Fabrication: A/Prof. Duk-Yong Choi, ANU

Advanced concept: Topological lasing

Using topologically protected states for lasing modes

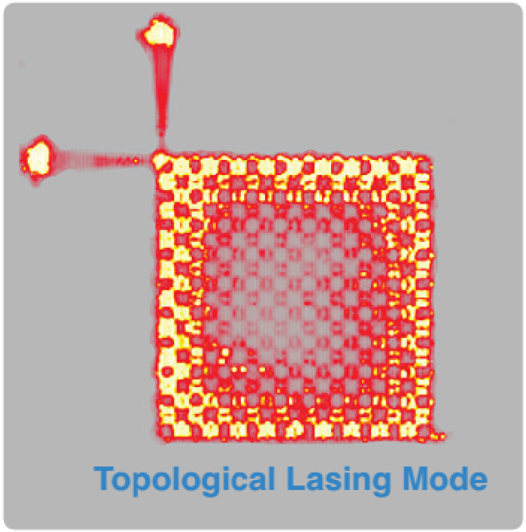

Array of micro-ring resonators pumped at the perimeter

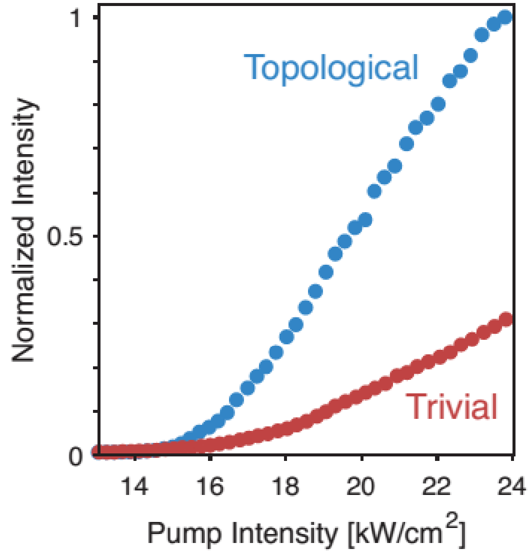

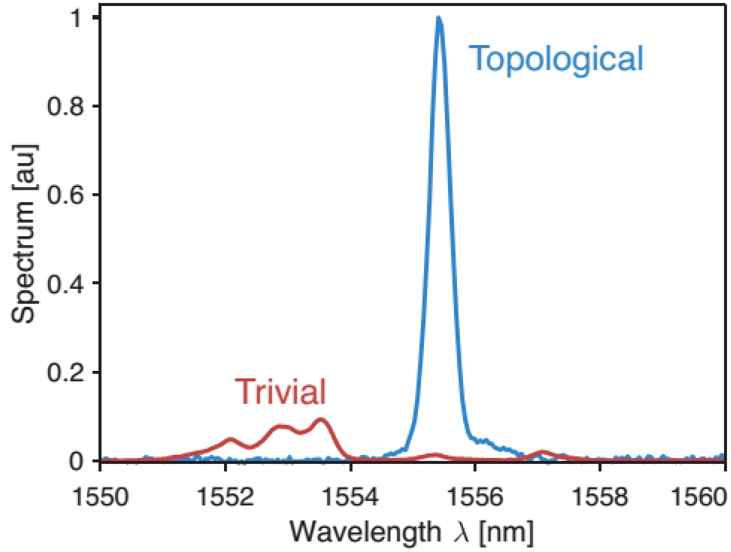

Achievement

- single-mode lasing via selective spatial pumping of the edge
- high slope efficiency
- coherent lasing
- robustness to local lattice deformations

Harari et al, Science **359**, eaar4003 (2018)
Bandres et al, Science **359**, eaar4005 (2018)

Challenges

Slow carrier dynamics in semiconductors is a source of instabilities

Topological cavities for nanolasing

- Close to the lasing threshold observations can be largely explained in terms of the physics of linear modes

- Topology provides a significant guiding scheme for the smart control of the number, spectral separation, localization scales and quality factors of edge and defect modes

- Control over radiation characteristics (generation of OAM, singular optics)

Active topological cavities

High-index III-V semiconductors
+ optical gain **+** topological field localization

Platform

Nanopatterned InGaAsP membranes with embedded quantum wells

Designs

VHE

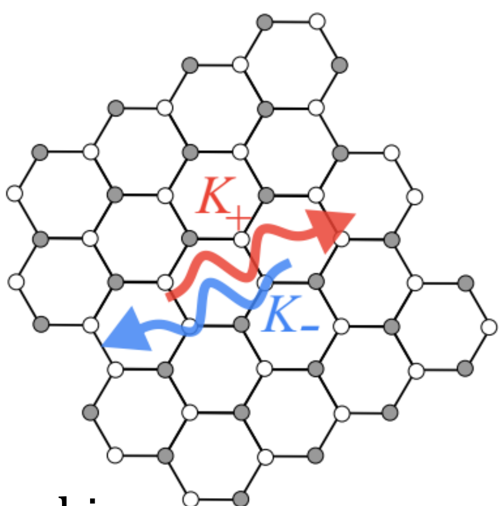

P-breaking

2D SSH

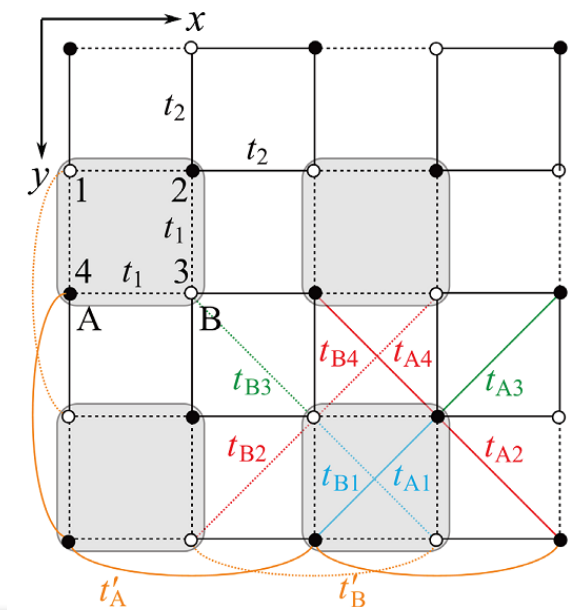

Valley-Hall nanophotonic cavities

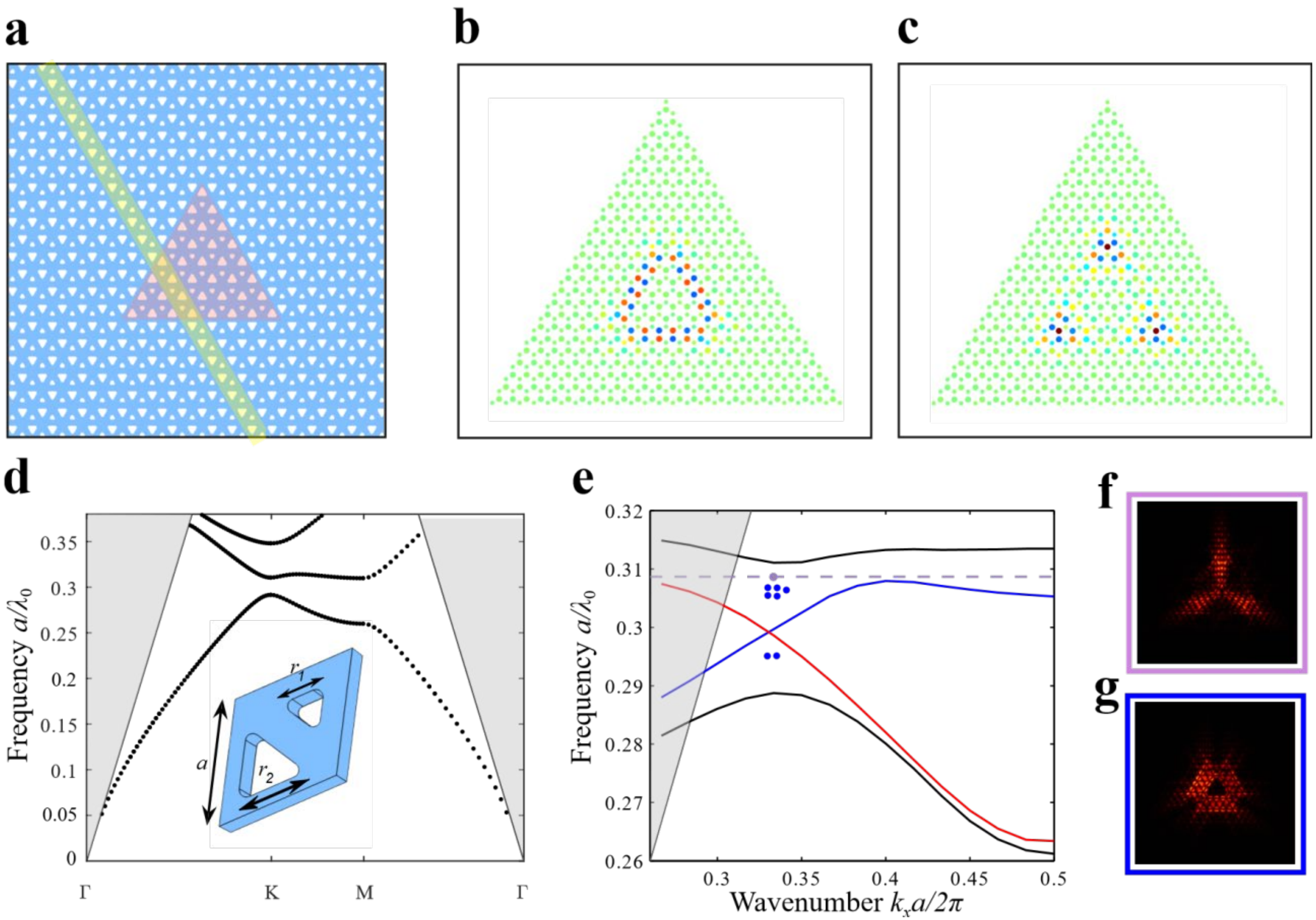

(**a**) Periodic lattice, cavity via inversion

(**b**,**c**) Tight-binding model

(**d**,**e**) Band structure

(**f**,**g**) Triade and edge cavity modes

Lasing from valley-Hall cavities

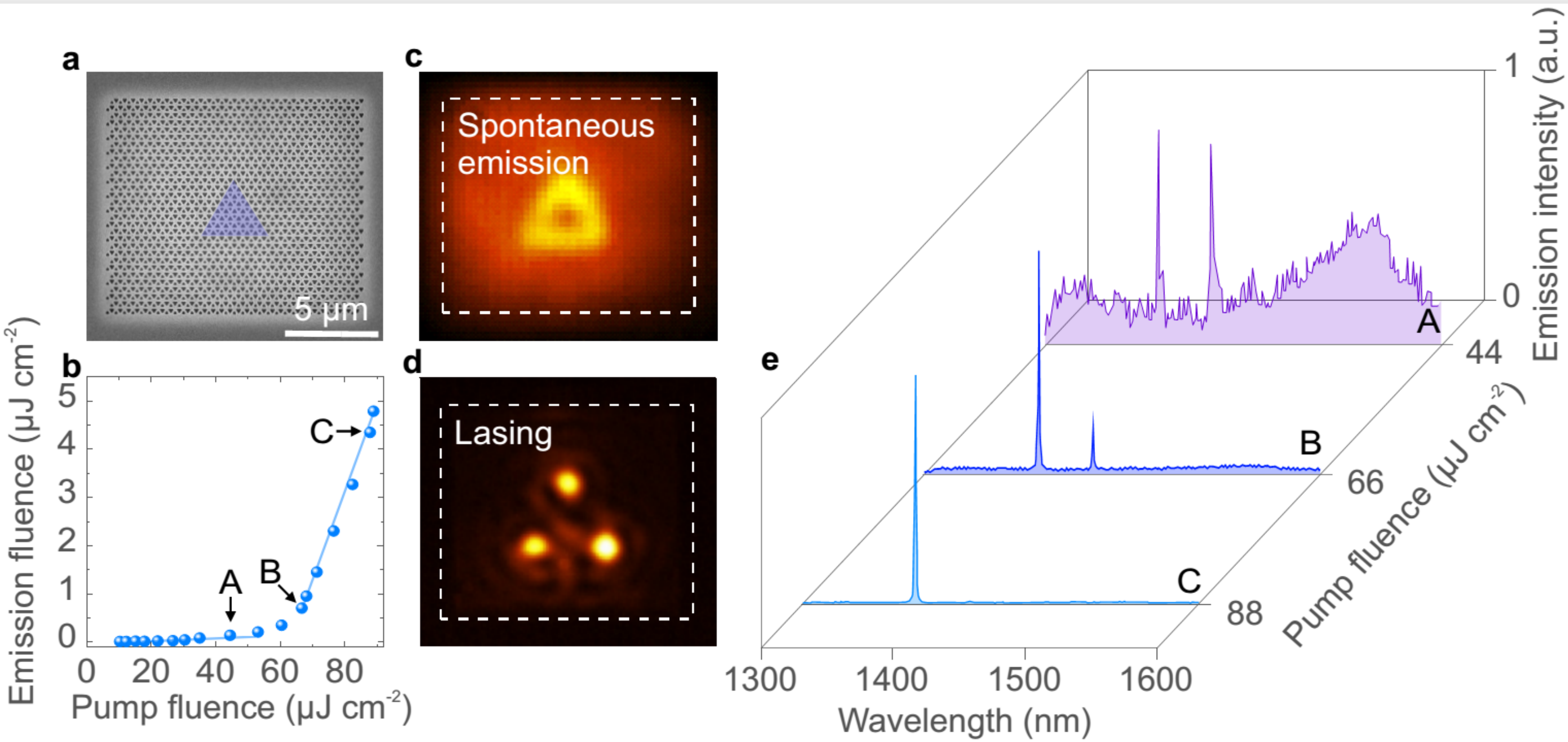

(**a**) SEM image of the fabricated sample. (**b**) Emission energy vs pump energy dependence showing a threshold transition to lasing. (**c**, **d**) Spatial distribution of emission for pump intensity (**c**) below and (**d**) above the lasing threshold. (**e**) Emission spectra showing a transition to a narrow-linewidth lasing.

Fabrication: Prof. Hong-Gyu Park's group, KU

Multipolar lasing modes from corner states

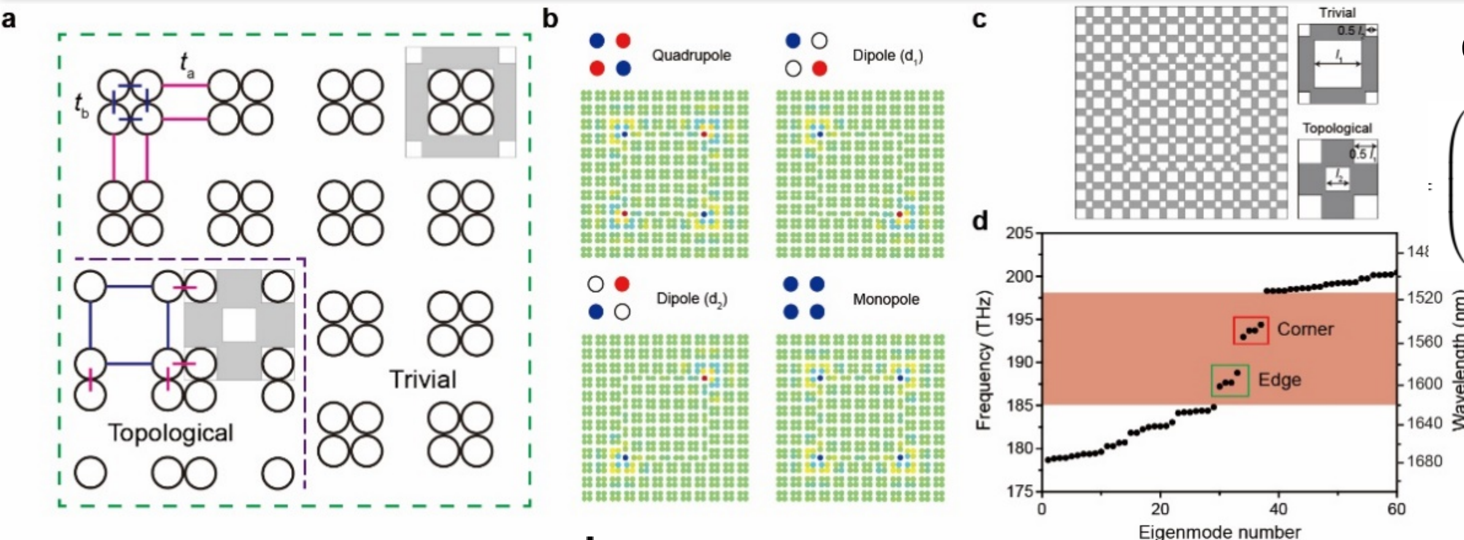

CMT Hamiltonian

$$\begin{pmatrix} \omega_c - i\gamma & -t_c & 0 & -t_c \\ -t_c & \omega_c - i\gamma & -t_c & 0 \\ 0 & -t_c & \omega_c - i\gamma & -t_c \\ -t_c & 0 & -t_c & \omega_c - i\gamma \end{pmatrix}$$

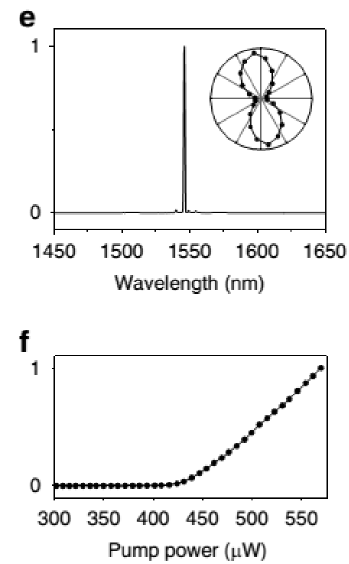

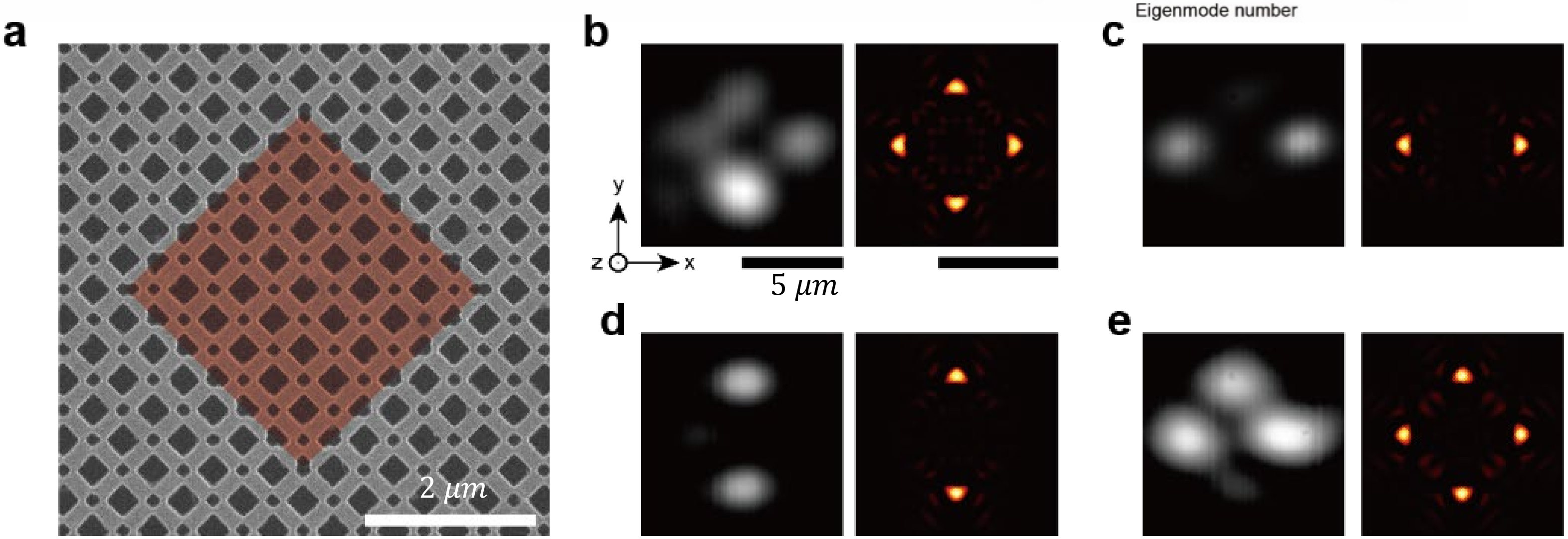

Fabrication: Prof. Hong-Gyu Park's group, KU

Links to other topics

- ✓ Structured light
- ✓ Singular optics
- ✓ Transformation optics
- ✓ Parity-Time symmetry
- ✓ Leaky wave theory

$$\hat{H} = (k_x\hat{\sigma}_x + k_y\hat{\sigma}_y)\hat{\tau}_z + m_1\hat{\tau}_x + m_2\hat{\tau}_y$$

$$\boldsymbol{m} = m_1 + im_2$$

Gao et al, Nature Nanotech. **15**, 1012 (2020)

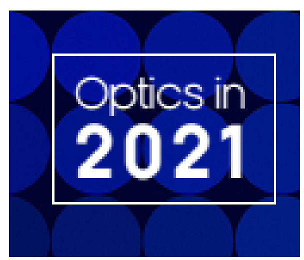

"Seeing topology using leaky photonic lattices", Optics & Photonics News, p. 50, December 2021

Leaky wave photonic lattices

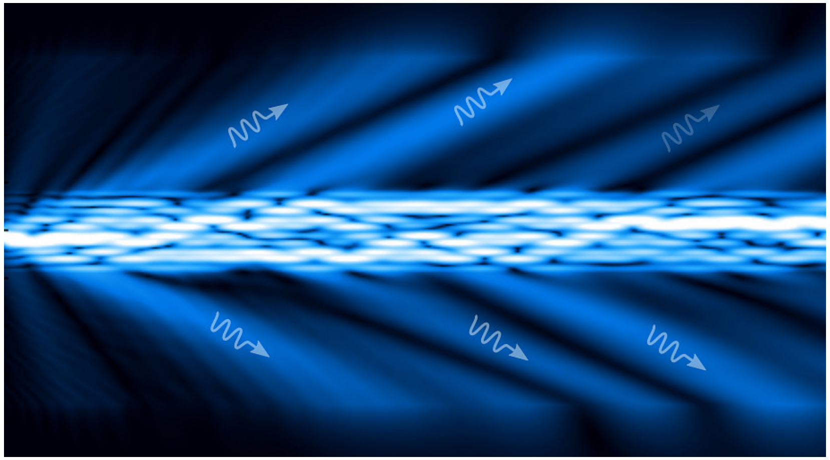

- Populate all modes at z = 0
- Design energy-dependent losses to empty upper band

Application: measuring bulk topological invariants

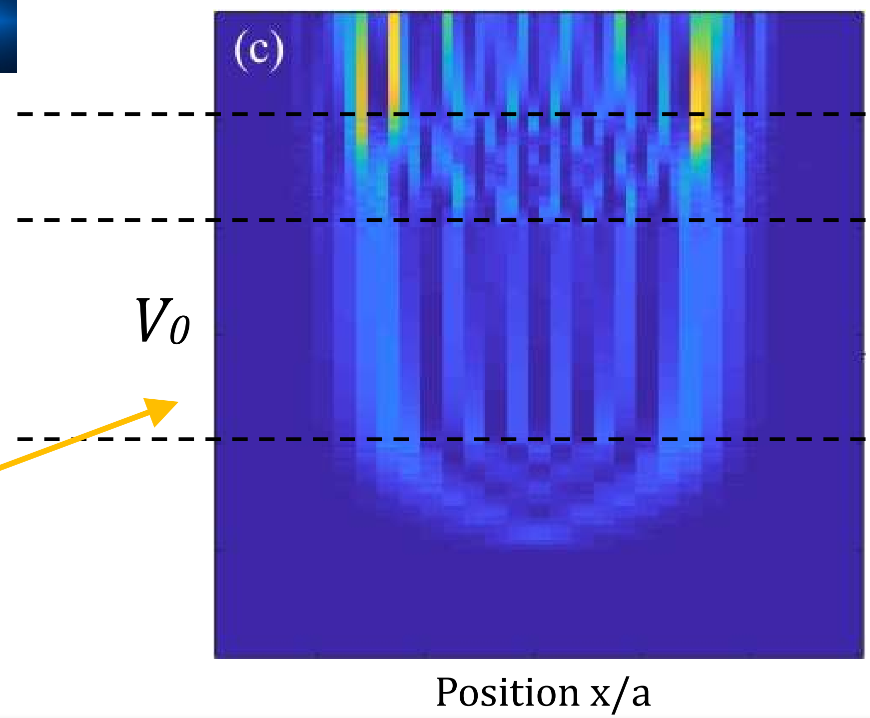

Insulating regime: observables insensitive to position of cutoff in band gap

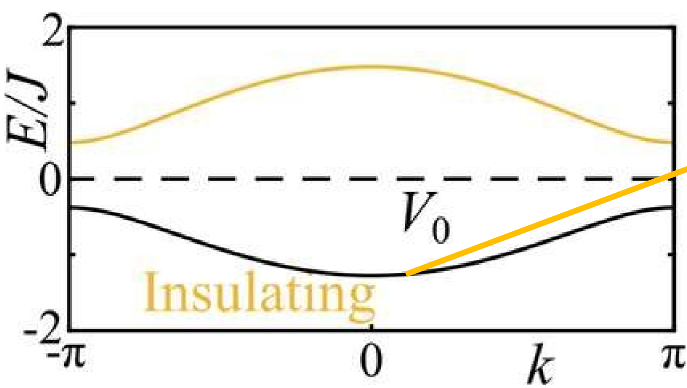

Leaky wave photonic lattices

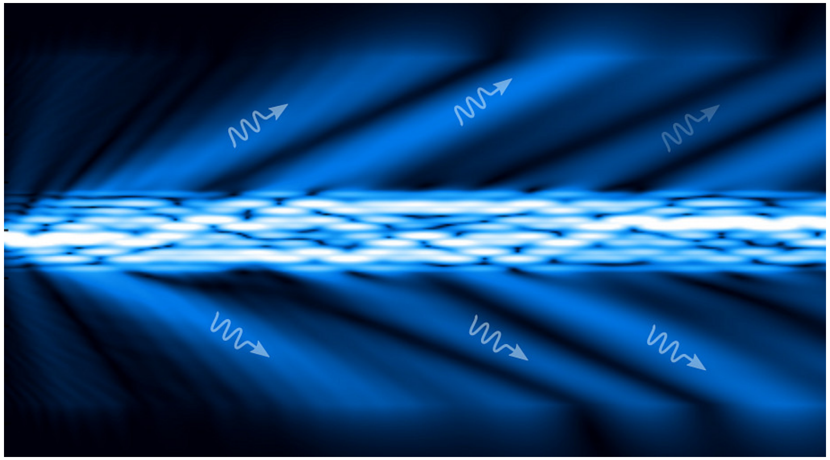

- Populate all modes at z = 0
- Design energy-dependent losses to empty upper band

Application: measuring bulk topological invariants

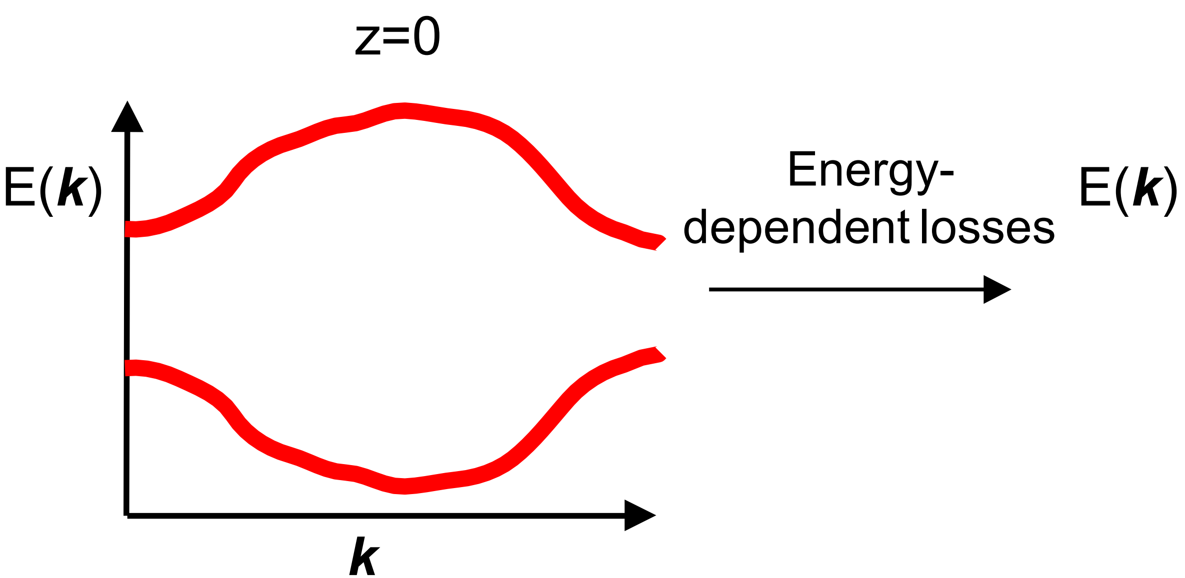

Implementation using silicon photonics

Device schematic

Upper & lower band eigenmodes

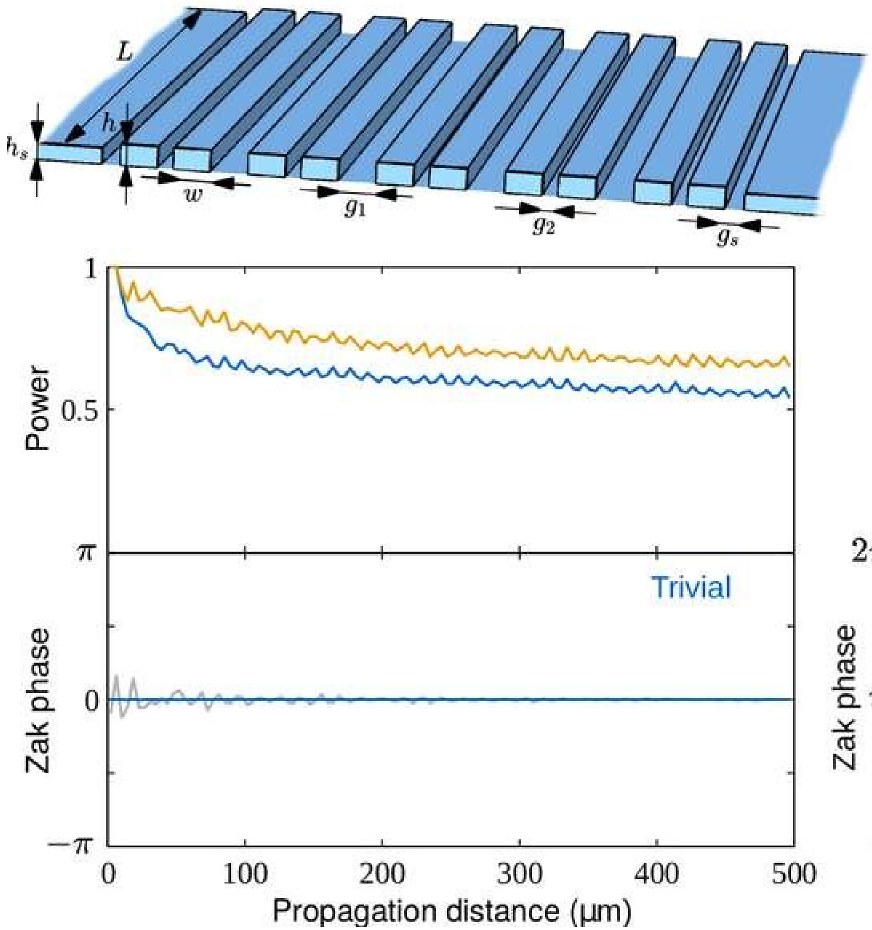

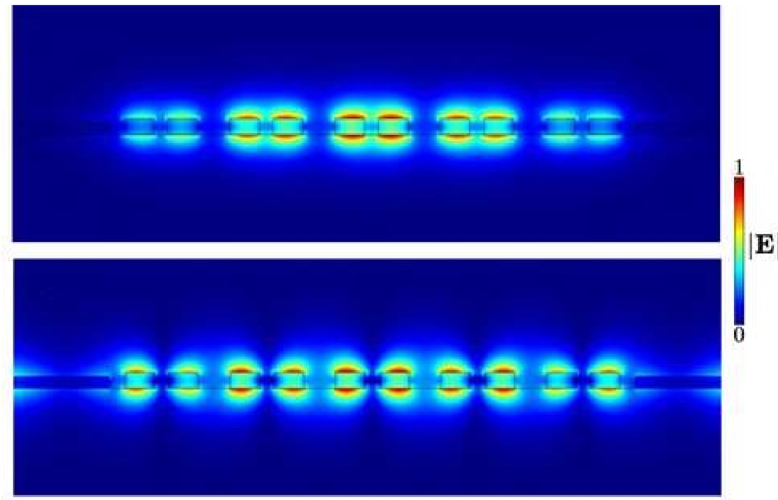

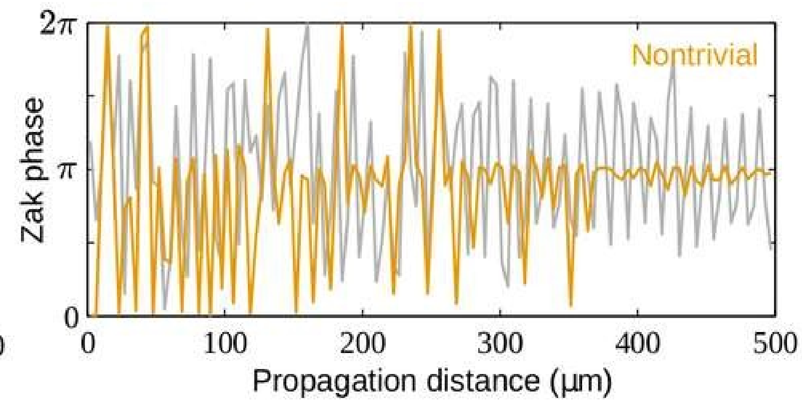

Work in progress: measure Zak phase in 1D Su-Schrieffer-Heeger model

Summary on topological nanophotonics

- ❑ The all-dielectric platform holds promise for robust generation and guiding of photons at the nanoscale, and the versatile design of *active topological metasurfaces* with integrated light sources

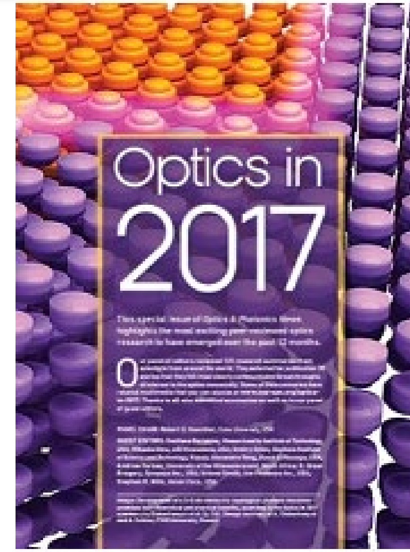

- ❑ Potential applications for the design of topological nanolasers with superior characteristics and tolerance to fabrication imperfections

- ❑ Physics governed by non-Hermitian and Dirac-like Hamiltonians

- ❑ Optical light trapping and nontrivial emission profiles

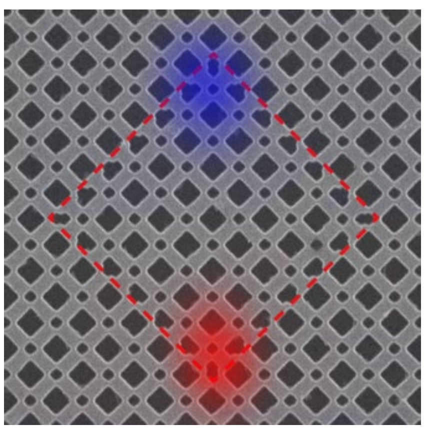

MIT Technology Review
Innovators Under 35
Asia Pacific

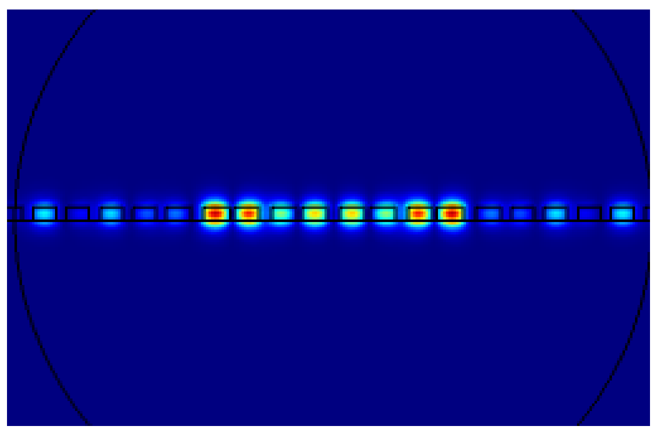

OPTICS & PHOTONICS NEWS DECEMBER 2021

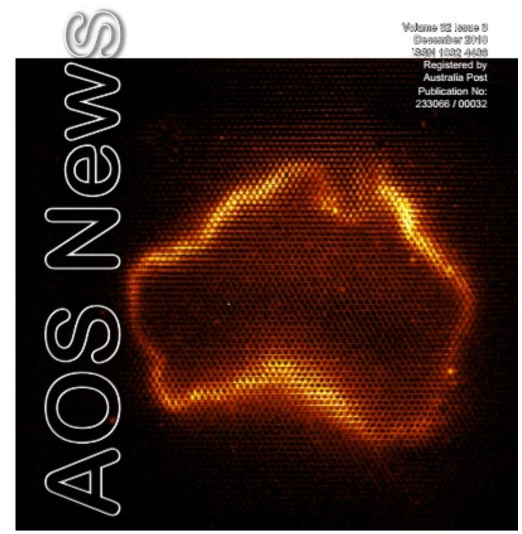

Nonlinear topological photonics

Lasers

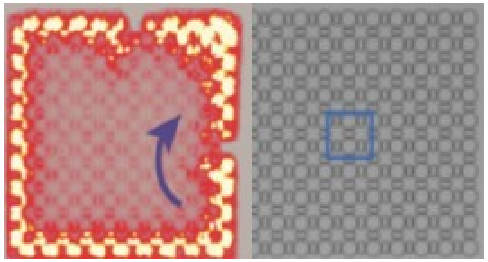

Science **359**, eaar4005 (2018)

Topological solitons

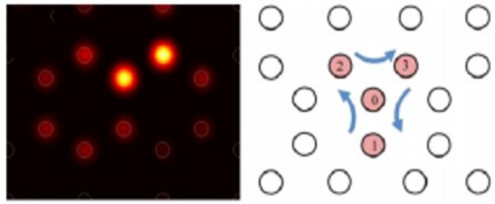

Phys. Rev. Lett. **111**, 243905 (2013)

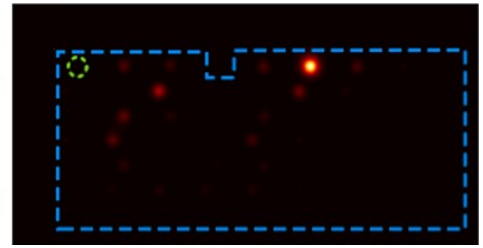

Phys. Rev. Lett. **117**, 143901 (2016)

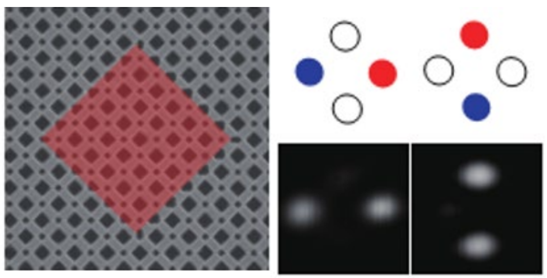

Nat. Commun. **11**, 5758 (2020)

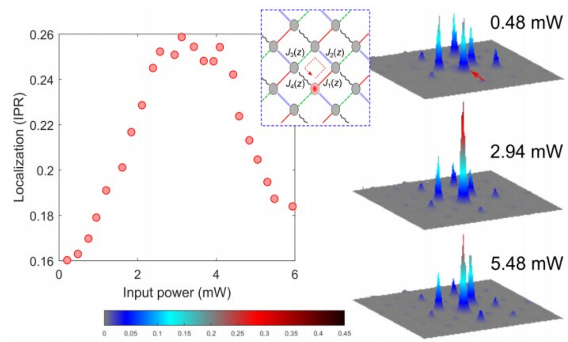

Science **368**, 856-859 (2020)

Nonlinear tunability, nonreciprocity, switching

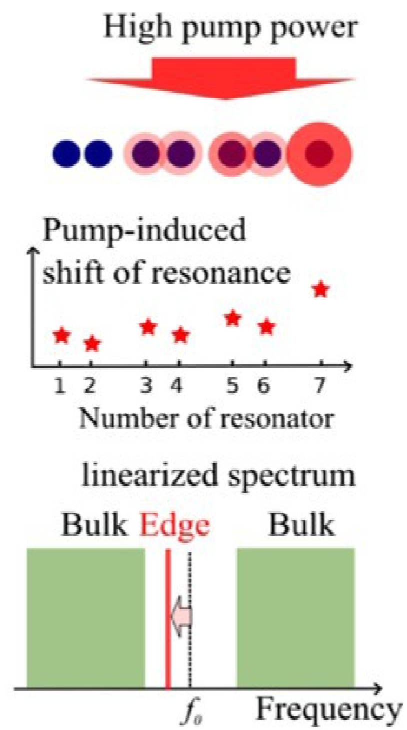

Phys. Rev. Lett. **121**, 163901 (2018)

Frequency conversion

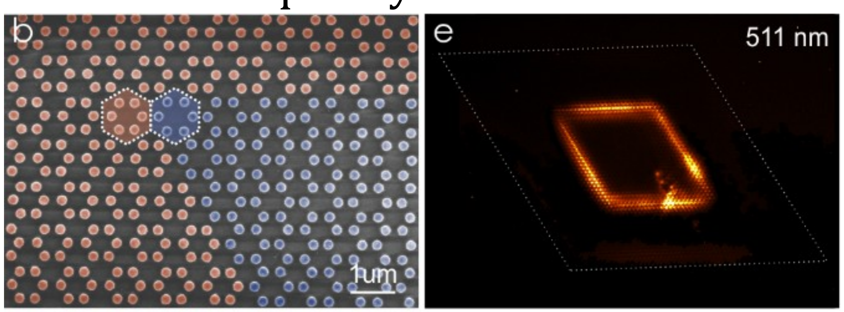

Phys. Rev. Lett. **123**, 103901 (2019)

Quantum light sources

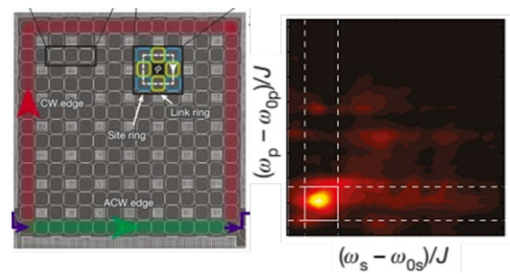

Nature **561**, 502 (2018)

Photonic waveguide lattices

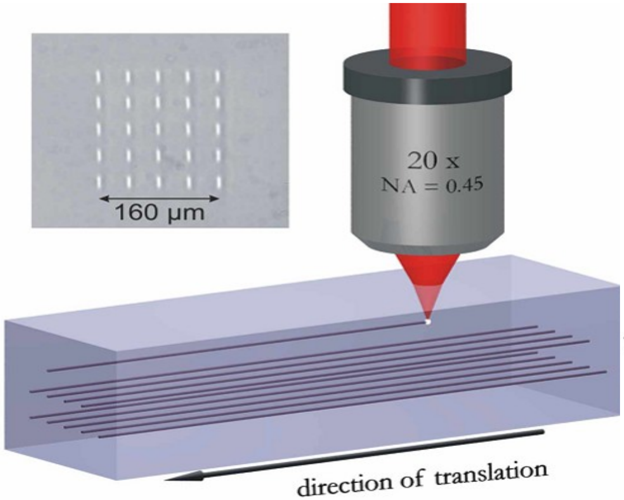

Optics Express **13**, 10552 (2005)
Optics Express **14**, 6055 (2006)

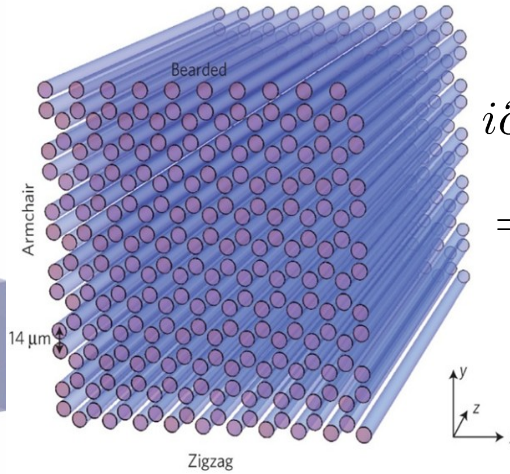

Nature Materials **13**, 57 (2014)

Paraxial equation:

$$i\partial_z\psi(\mathbf{r},z) =$$
$$= -\frac{1}{2k_0}\nabla^2_{\mathbf{r}}\psi(\mathbf{r},z) - \frac{k_0\Delta n(\mathbf{r})}{n_0}\psi(\mathbf{r},z);$$

Coupled-mode equation:

$$i\partial_z\psi_i(z) = \beta_i\psi_i + \sum_j c_{ij}(\lambda)\psi_j(z);$$

Optical Kerr nonlinearity:

$$n_{\text{eff}} = n_{\text{lin}} + n_2 I.$$

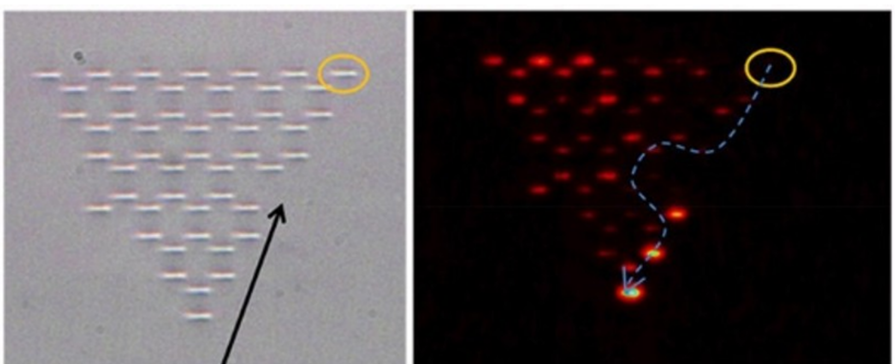

defect

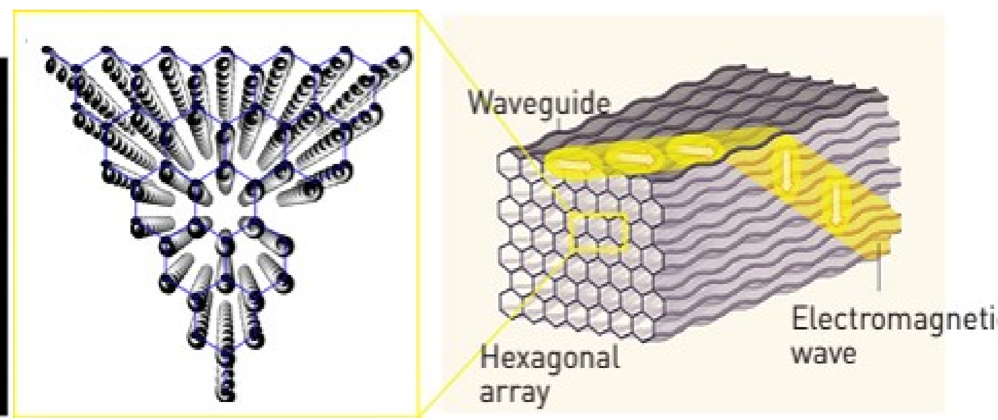

Nature **496**, 196 (2013)

Topological solitons

Bulk solitons | **Edge solitons**

Numerics

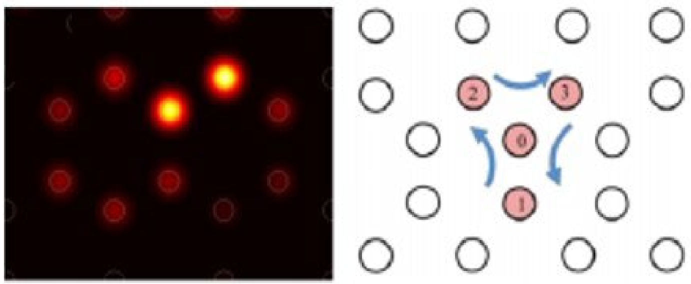

Lumer et al, Phys. Rev. Lett. **111**, 243905 (2013)

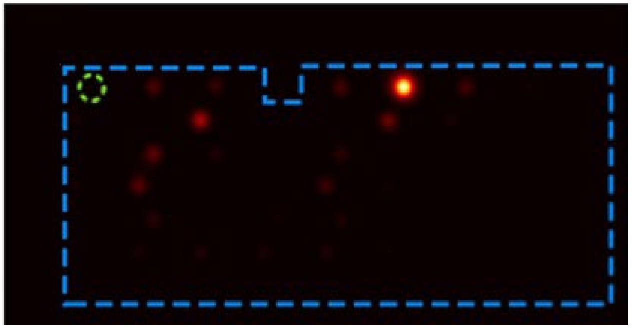

Leykam & Chong, Phys. Rev. Lett. **117**, 143901 (2016)

Experiments

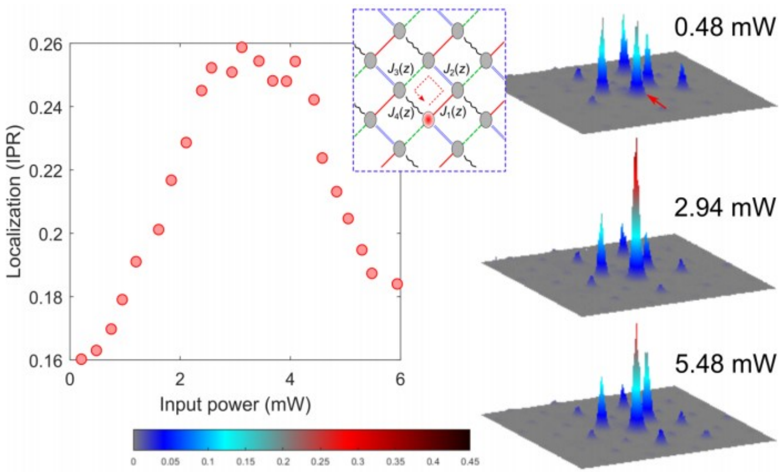

Mukherjee & Rechtsman, Science **368**, 856-859 (2020)

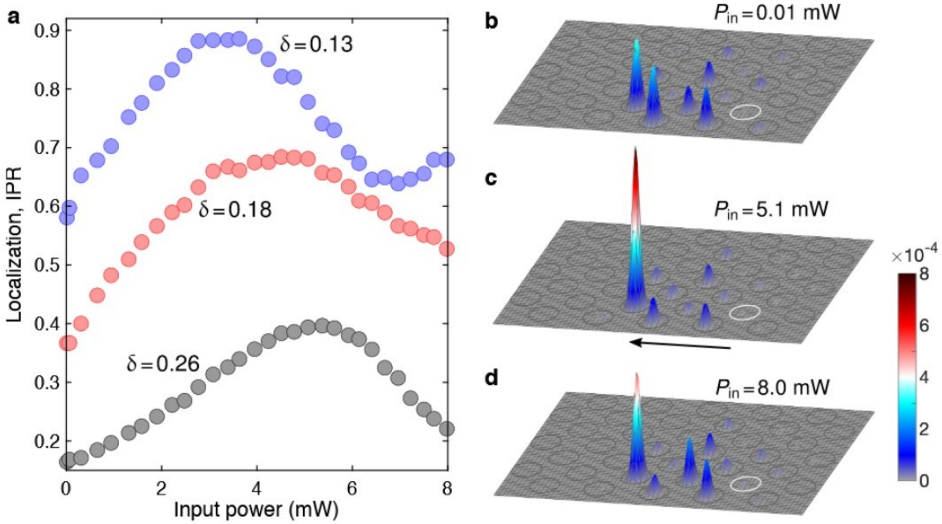

Mukherjee & Rechtsman, arXiv:2010.11359

Maczewsky et al, Science **370** (6517), 701 (2020)

Nonlinear Dirac model

Nonlinear generalizations of topological lattice models

$$i\partial_z \mathbf{\Psi} = (\hat{H} + \hat{H}_{NL})\mathbf{\Psi}$$

Su-Schrieffer-Heeger (SSH) model:

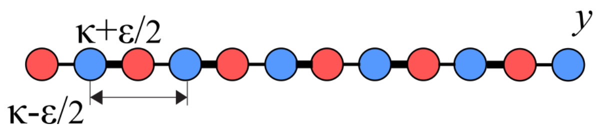

$$\hat{H}_D(\delta k) = -\varepsilon\hat{\sigma}_x + v_D\hat{\sigma}_y\delta k$$

Staggered graphene:

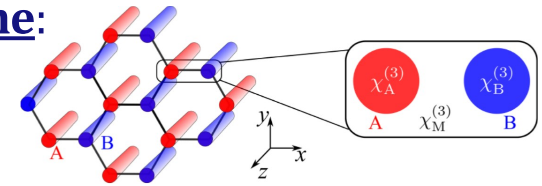

$$\hat{H}_D(\delta \boldsymbol{k}) = \delta k_x\hat{\sigma}_x + \delta k_y\hat{\sigma}_y + M\hat{\sigma}_z$$

- Models universal continuum (long wavelength) dynamics in topological lattices
- Analytical solutions for stationary localized states (bulk and edge solitons)
- Captures the nontrivial spin properties

$$i\partial_t \boldsymbol{\psi} = \begin{pmatrix} M - g|\psi_1|^2 - \beta\left[\partial_x^2 + \partial_y^2\right] & -i\partial_x - \partial_y - \eta\left(-i\partial_x + \partial_y\right)^2 \\ -i\partial_x + \partial_y - \eta\left(i\partial_x + \partial_y\right)^2 & -M - g|\psi_2|^2 + \beta\left[\partial_x^2 + \partial_y^2\right] \end{pmatrix}\boldsymbol{\psi}$$

valley-Hall insulator ($\beta = 0$); Bernevig–Hughes–Zhang model ($\eta = 0$)

Topological gap solitons and nonlinear edge states

Su-Schrieffer-Heeger (SSH) model:

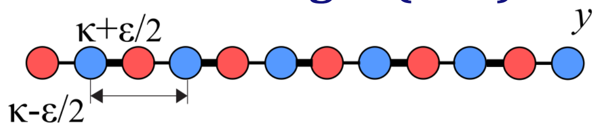

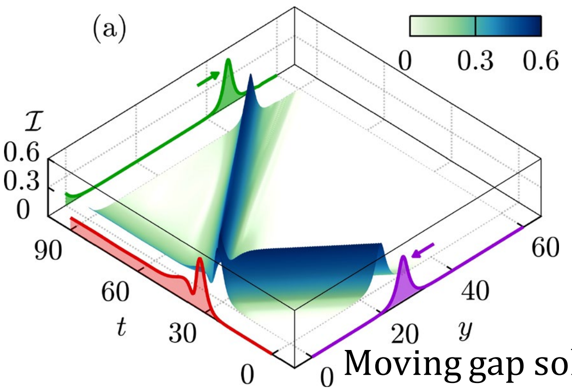

Moving gap solitons are capable of exciting edge states by reflecting of topological interfaces

trivial **nontrivial**

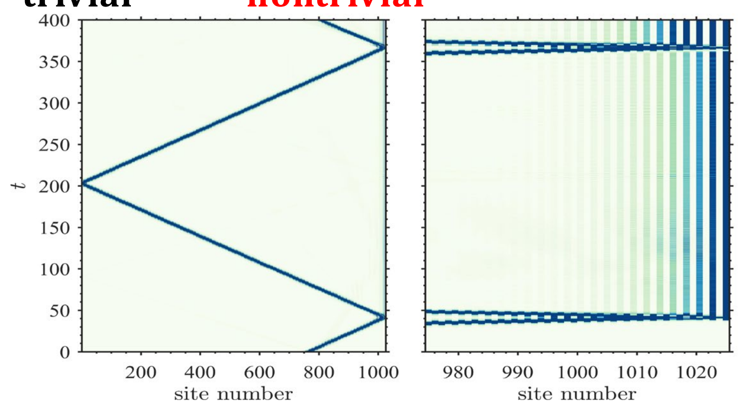

Nonlinear coupling to topological modes

Staggered graphene:

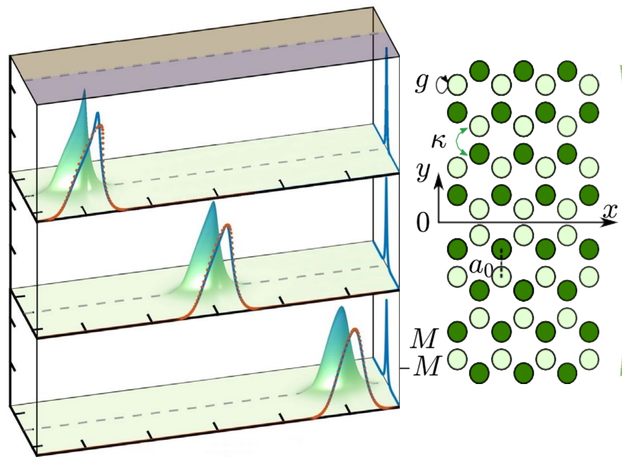

Gradient catastrophe of edge pulses

Phys. Rev. Research, in press

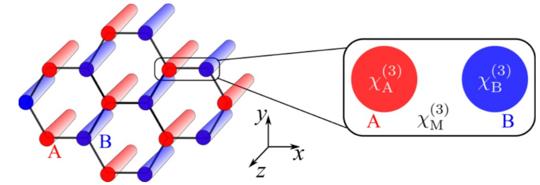

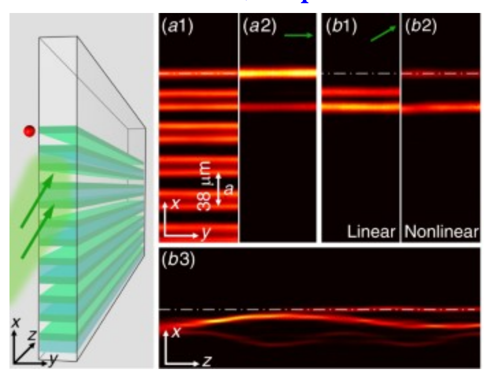

Experiment by Prof. Zhigang Chen group

Light: Science & Applications **9**, 147 (2020)

Semivortex solitons and chiral edge states

Laser & Photon. Rev. **13**, 1900223 (2019)

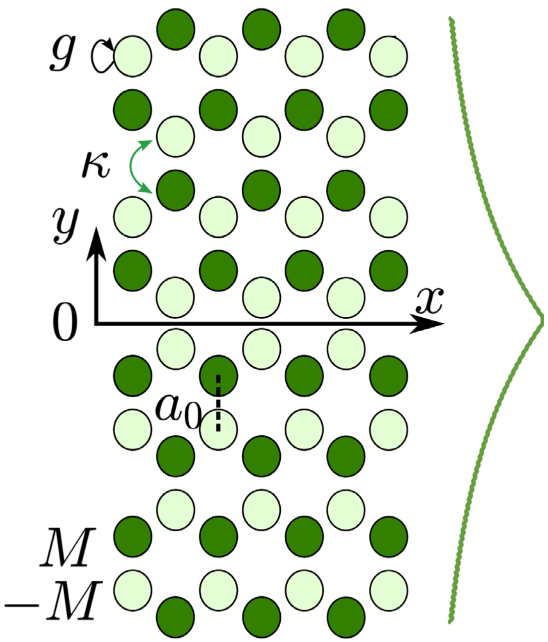

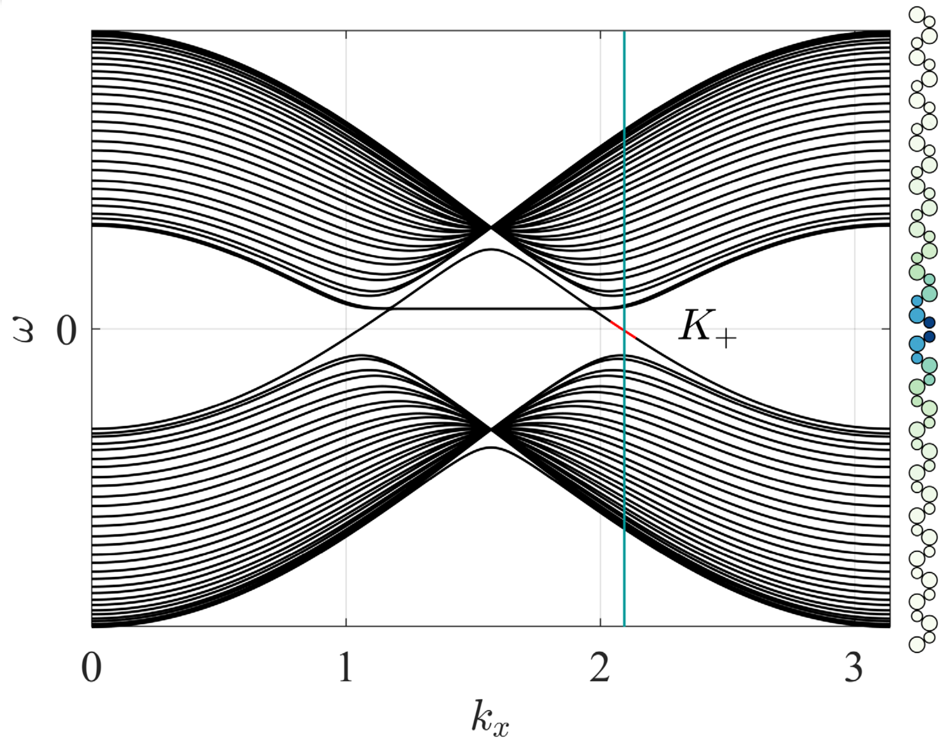

Dirac equations
for a spinor wave function near K_+
$(|M| \ll \kappa;\ v_D = \frac{3}{2}\kappa a_0 = 1;\ t = z/v_D)$:

$$i\partial_t \boldsymbol{\psi} = \hat{H}_D(\delta\boldsymbol{k})\boldsymbol{\psi};\ \delta\boldsymbol{k} = (\delta k_x, \delta k_y) \equiv -i\,(\partial_x, \partial_y);$$

$$\boxed{\hat{H}_D(\delta\boldsymbol{k}) = \delta k_x \hat{\sigma}_x + \delta k_y \hat{\sigma}_y + M\hat{\sigma}_z.}$$

$$M(y) = \begin{cases} M_0, & y > 0; \\ -M_0, & y < 0. \end{cases}$$

Dispersion of *edge states*:

$$\boxed{\omega = -\delta k_x\ (M_0 > 0).}$$

Structure of the *edge wavepacket*:

$$\boldsymbol{\psi} = a_0(x+t)e^{-M_0|y|}e^{i\omega(x+t)}\begin{pmatrix} 1 \\ -1 \end{pmatrix}.$$

Nonlinear edge waves

$$i\partial_t \boldsymbol{\psi} = \begin{pmatrix} M - g|\psi_1|^2 & -i\partial_x - \partial_y \\ -i\partial_x + \partial_y & -M - g|\psi_2|^2 \end{pmatrix} \boldsymbol{\psi},$$

$$\xrightarrow{\psi = \psi e^{ikx}} \begin{pmatrix} \psi_1(y,t) \\ \psi_2(y,t) \end{pmatrix} = \sqrt{2\varrho_s(y)} \times \begin{pmatrix} \cos\alpha_s(y) \\ -\sin\alpha_s(y) \end{pmatrix} e^{-i\omega t + ikx}.$$

$$\alpha_n(y+y_0) = = \arctan\left[\frac{\Omega - \omega}{\sqrt{\Omega^2 - \omega^2}} \tanh\left(\sqrt{\Omega^2 - \omega^2}\,(y+y_0)\right)\right];$$

$$\varrho_s(\alpha_s) = \frac{2\left(-k\sin 2\alpha_s - \omega + M_0\cos 2\alpha_s\right)}{g\left(1 + \cos^2 2\alpha_s\right)};$$

$$\delta = \arctan\frac{k}{M_0}, \quad \Omega = \sqrt{M_0^2 + k^2},$$

$$\alpha_s = \alpha_n - \delta/2.$$

Nonlinear edge state's profile:

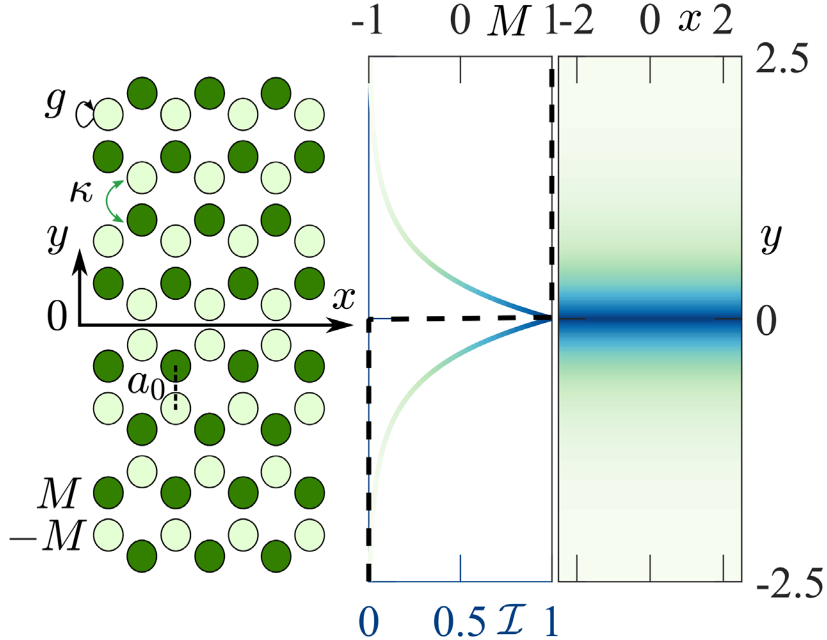

The nonlinear dispersion for edge states:

$$\omega + k = -gI_1/2,\; I_1 = |\psi_1(y=0)|^2.$$

Intensity: $\mathcal{I} = |\psi_1(y)|^2 + |\psi_2(y)|^2.$

Boundary condition: $\psi_1(0) = -\psi_2(0).$

Smirnova et al, Laser & Photon. Rev. **13**, 1900223 (2019)

Nonlinear edge waves

$$\boxed{i\partial_t\boldsymbol{\psi} = \begin{pmatrix} M - g|\psi_1|^2 & -i\partial_x - \partial_y \\ -i\partial_x + \partial_y & -M - g|\psi_2|^2 \end{pmatrix}\boldsymbol{\psi},} \xRightarrow{\psi = \psi e^{ikx}} \begin{pmatrix} \psi_1(y,t) \\ \psi_2(y,t) \end{pmatrix} = \sqrt{2\varrho_s(y)}$$

$$\times \begin{pmatrix} \cos\alpha_s(y) \\ -\sin\alpha_s(y) \end{pmatrix} e^{-i\omega t + ikx}.$$

$$\Downarrow$$

Integral characteristics

Integral power: $\mathcal{P} = \int_0^\infty \langle\boldsymbol{\psi}|\boldsymbol{\psi}\rangle dy = \dfrac{\pi}{g\sqrt{2}} + \dfrac{\sqrt{2}}{g}\arctan\left(\dfrac{-k\omega + M_0\sqrt{\Omega^2-\omega^2}}{\sqrt{2}[M_0\omega + k\sqrt{\Omega^2-\omega^2}]}\right).$

Integral spin: $\langle S_x\rangle = \dfrac{1}{2}\int_0^\infty \langle\boldsymbol{\psi}|\ \hat{\sigma}_x|\boldsymbol{\psi}\rangle dy$

$$\boxed{\langle S_x\rangle = -\frac{1}{g}\arcsin\left[\frac{1}{\sqrt{2}}\sin\left(\mathcal{P}\frac{g}{\sqrt{2}}\right)\right].}$$

Nonlinear dynamics of edge states

$$i\partial_t \boldsymbol{\psi} = \begin{pmatrix} M - g|\psi_1|^2 & -i\partial_x - \partial_y \\ -i\partial_x + \partial_y & -M - g|\psi_2|^2 \end{pmatrix} \boldsymbol{\psi}.$$

For transversely localized solutions:

$$\frac{\partial \mathcal{P}}{\partial t} = -2\frac{\partial \langle S_x \rangle}{\partial x};$$
$$\frac{\partial \mathcal{P}}{\partial t} = -2\frac{d \langle S_x \rangle}{d\mathcal{P}} \frac{\partial \mathcal{P}}{\partial x},$$

For edge states:

$$\langle S_x \rangle = \langle S_x \rangle (\mathcal{P});$$
$$\mathcal{P} = \mathcal{P}(\omega, k);$$
$$\omega + k = -gI_1/2,$$

$$\Downarrow$$

Nonlinear simple wave equation for the intensity at the domain wall for small nonlinearity :

$gI_1 \ll M_0$: $\boxed{\partial_t I_1 - \partial_x I_1 \left(1 - g^2 I_1^2 / \left(4M_0^2\right)\right) = 0.}$

Gradient catastrophe

For the initial Gaussian profile $f_0(x) = F_0 e^{-x^2/\Lambda_0^2}$:

the discontinuity formation time: $\boxed{t^* = 2\sqrt{e}\frac{M_0^2}{g^2 F_0^2}\Lambda_0}$.

Asymptotic methods

$$i\partial_t\boldsymbol{\psi} = \begin{pmatrix} M - g|\psi_1|^2 & -i\partial_x - \partial_y - \eta\left(-i\partial_x + \partial_y\right)^2 \\ -i\partial_x + \partial_y - \eta\left(i\partial_x + \partial_y\right)^2 & -M - g|\psi_2|^2 \end{pmatrix}$$

Small parameter $\mu \ll 1$: $\mu \sim gI_1/M_0,\ \eta M_0 \sim \mu^2,\ \tau_n = \mu^n t,\ \xi \equiv x + t.$

$$\psi_{1,2}(x,y,t) = \pm a(\xi;\tau_n)e^{-M_0|y|} + \sum_{n=1}^{\infty}\mu^n \psi_{1,2}^{(n)}\left(y;\xi;\tau_n\right).$$

Evolution equation for the edge pulse with accuracy $\sim \mu^2$:

$$\boxed{i\left(\partial_t a + \frac{g^2|a|^2}{32M_0^2}a\partial_\xi|a|^2\right) + \frac{g}{4}|a|^2 a + \eta\left(\partial_{\xi\xi}a - M_0^2 a\right) = 0.}$$

Neglecting spatial dispersion $\eta = 0$:

$$\frac{\partial|a|}{\partial\tau_2} + \frac{g^2}{16M_0^2}|a|^4\frac{\partial|a|}{\partial\xi} = 0\,,$$

Taking into account $\sqrt{2I_1} \equiv |a|$, we obtain the previously found *simple wave equation*

$$\Downarrow$$

$$\boxed{\partial_t I_1 - \partial_x I_1\left(1 - g^2 I_1^2/\left(4M_0^2\right)\right) = 0.}$$

Nonlinear dynamics

- $$\frac{\partial I_1}{\partial t} - \frac{\partial I_1}{\partial x}\left(1 - \frac{g^2 I_1^2}{4M_0^2}\right) = 0.$$
- $$i\frac{\partial a}{\partial t} = -\frac{g}{4}|a|^2 a - i\frac{g^2}{32M_0^2}|a|^2\frac{\partial |a|^2}{\partial \xi}a - \eta\frac{\partial^2 a}{\partial \xi^2} + M_0^2\eta a\,.$$

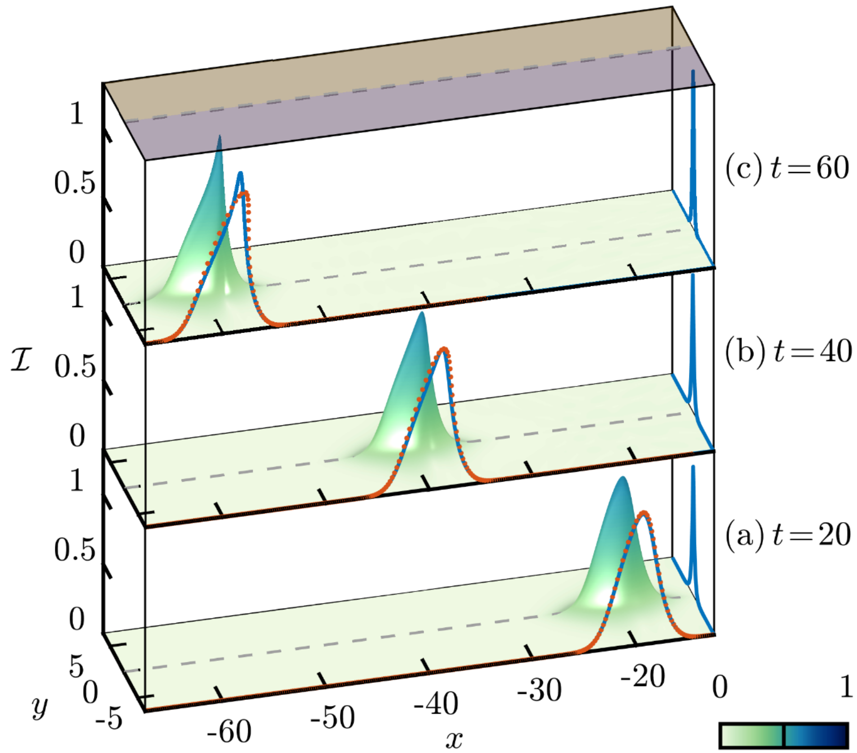

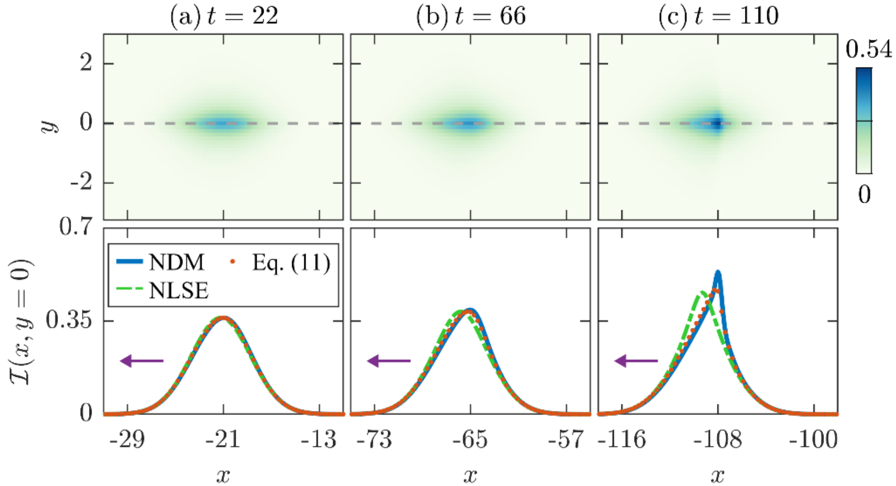

As the pulse propagates its tail becomes increasingly steep. Modified NLSE correctly reproduces the growing asymmetry.

Edge solitons

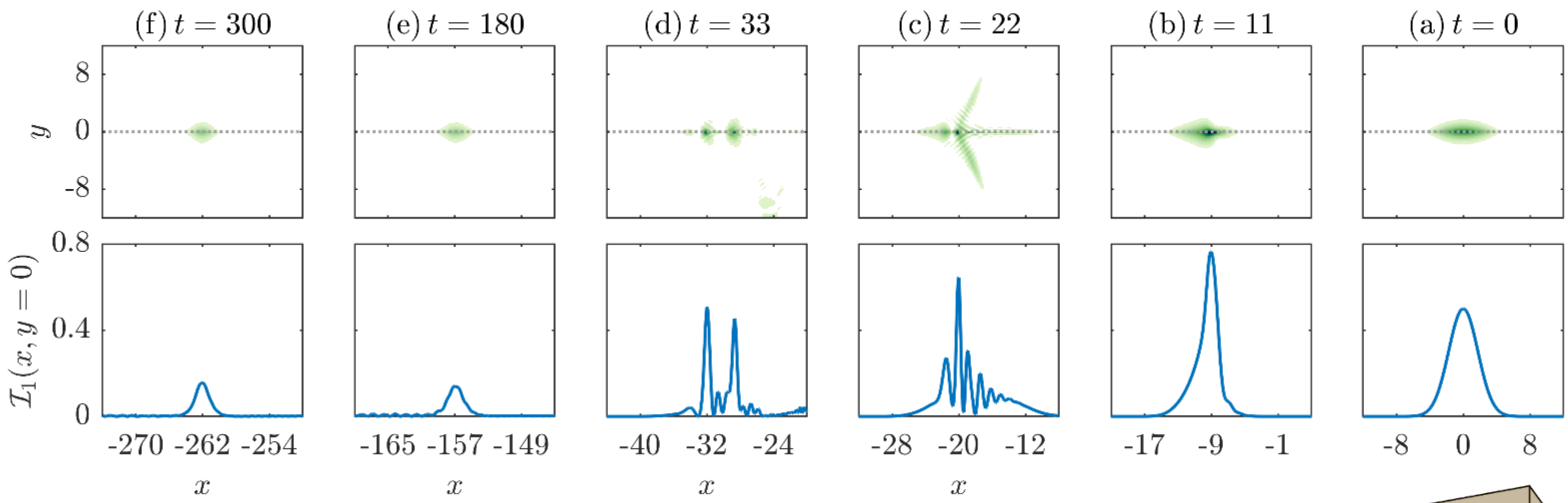

Self-steepening leads to the break-up of wide pulses, resulting in the radiation of part of its energy into bulk modes, with the remainder forming a quasi-soliton. The edge soliton is capable of traversing sharp bends.

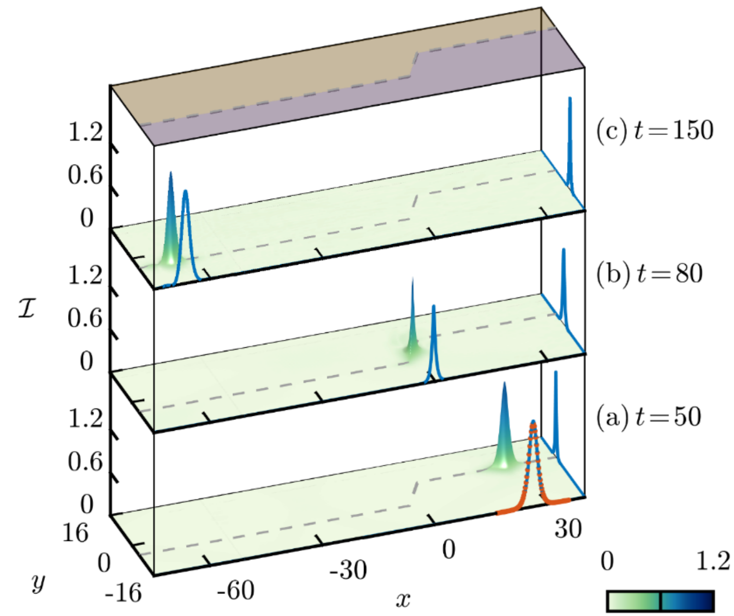

Valley-Hall domain wall in waveguide arrays

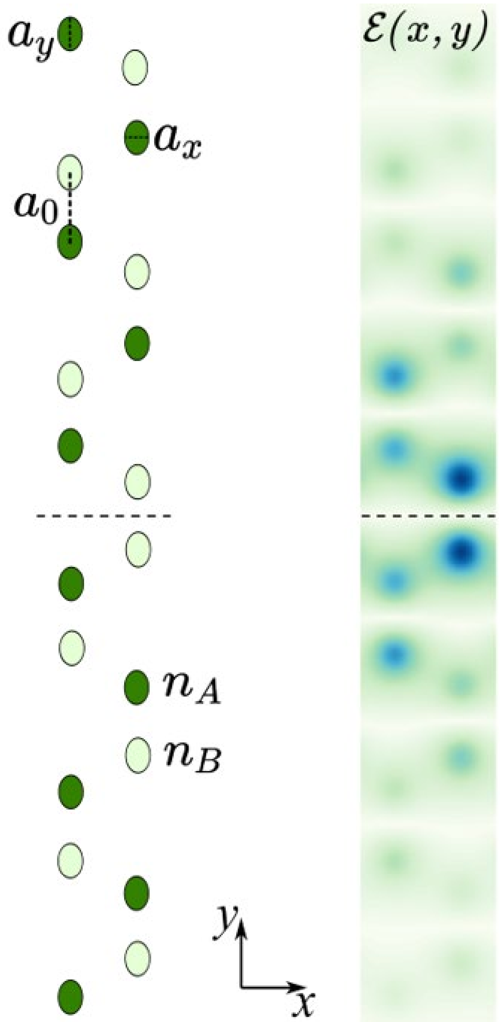

Lattice geometry Edge state

Paraxial equation :

$$i\frac{\partial \mathcal{E}}{\partial z} + \frac{1}{2k_0}\Delta_\perp \mathcal{E} + \frac{k_0\left(n_L(x,y) + n_2|\mathcal{E}|^2\right)}{n_0}\mathcal{E} = 0.$$

Parameter	Value
a_x	3.2 μm
a_y	4.9 μm
a_0	19 μm
a	$\sqrt{3}a_0$
n_0	1.47
n_A	2.6×10^{-3}
n_B	2.8×10^{-3}
n_2	3×10^{-20} m^2/W
λ	1650 nm
I_0	10^{16} W/m^2

Phys. Rev. Lett. **120**, 063902 (2018)

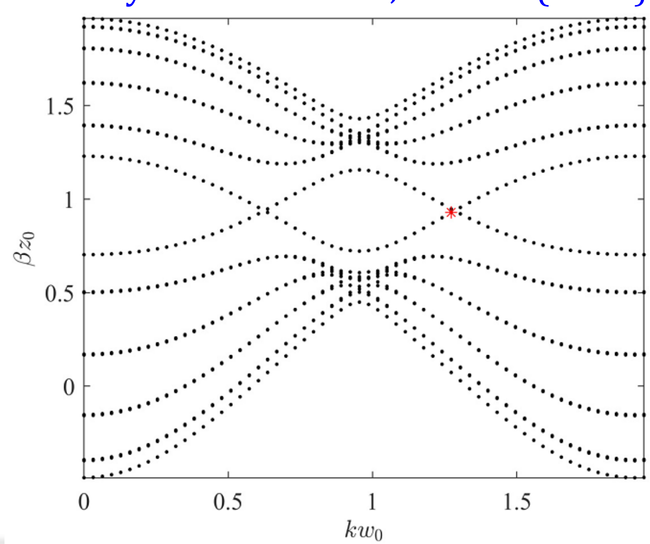

Beam propagation

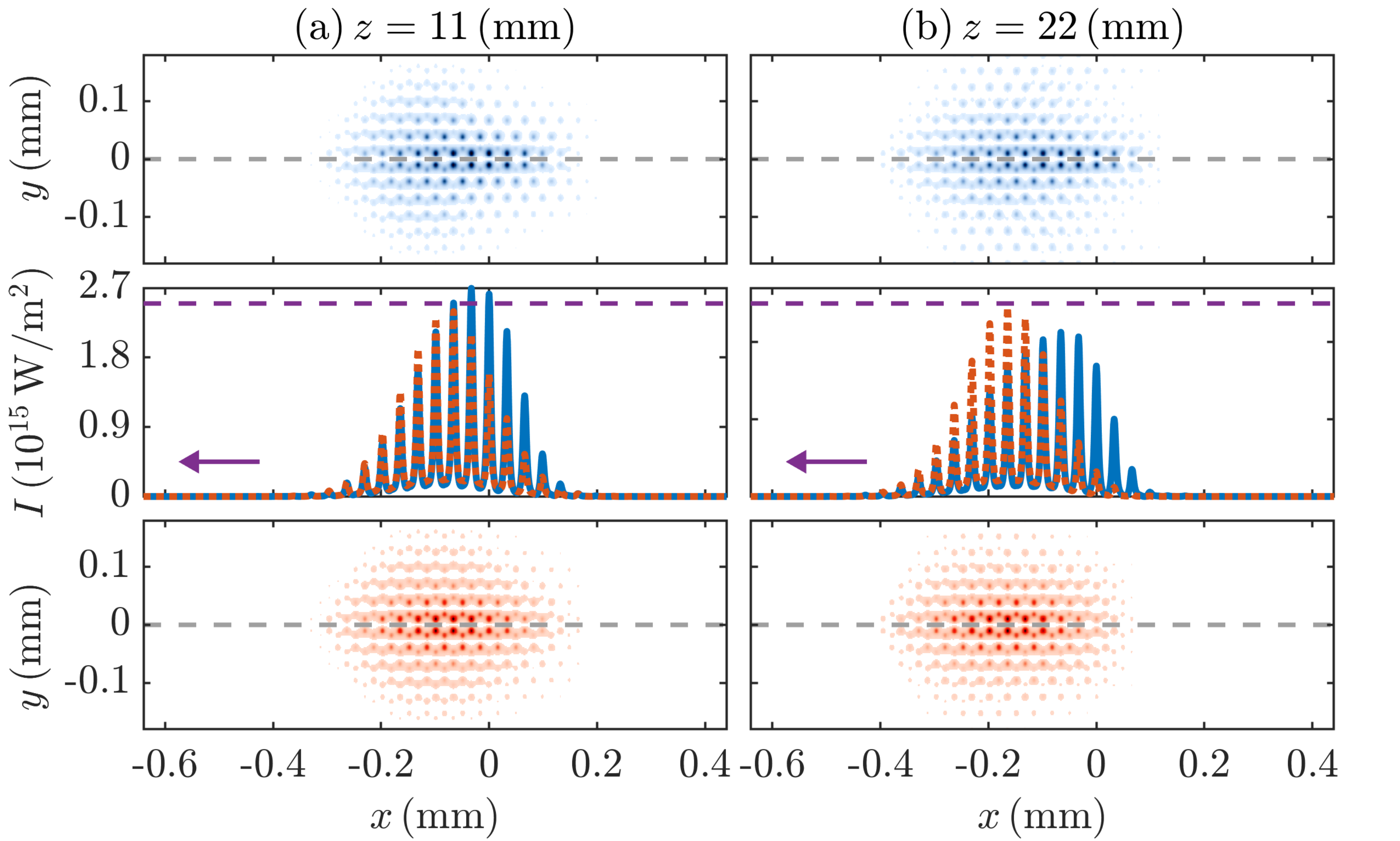

Beam propagation

Intensity distribution at the interface obtained in modeling of the paraxial equation (left) and the corresponding Dirac model (right)

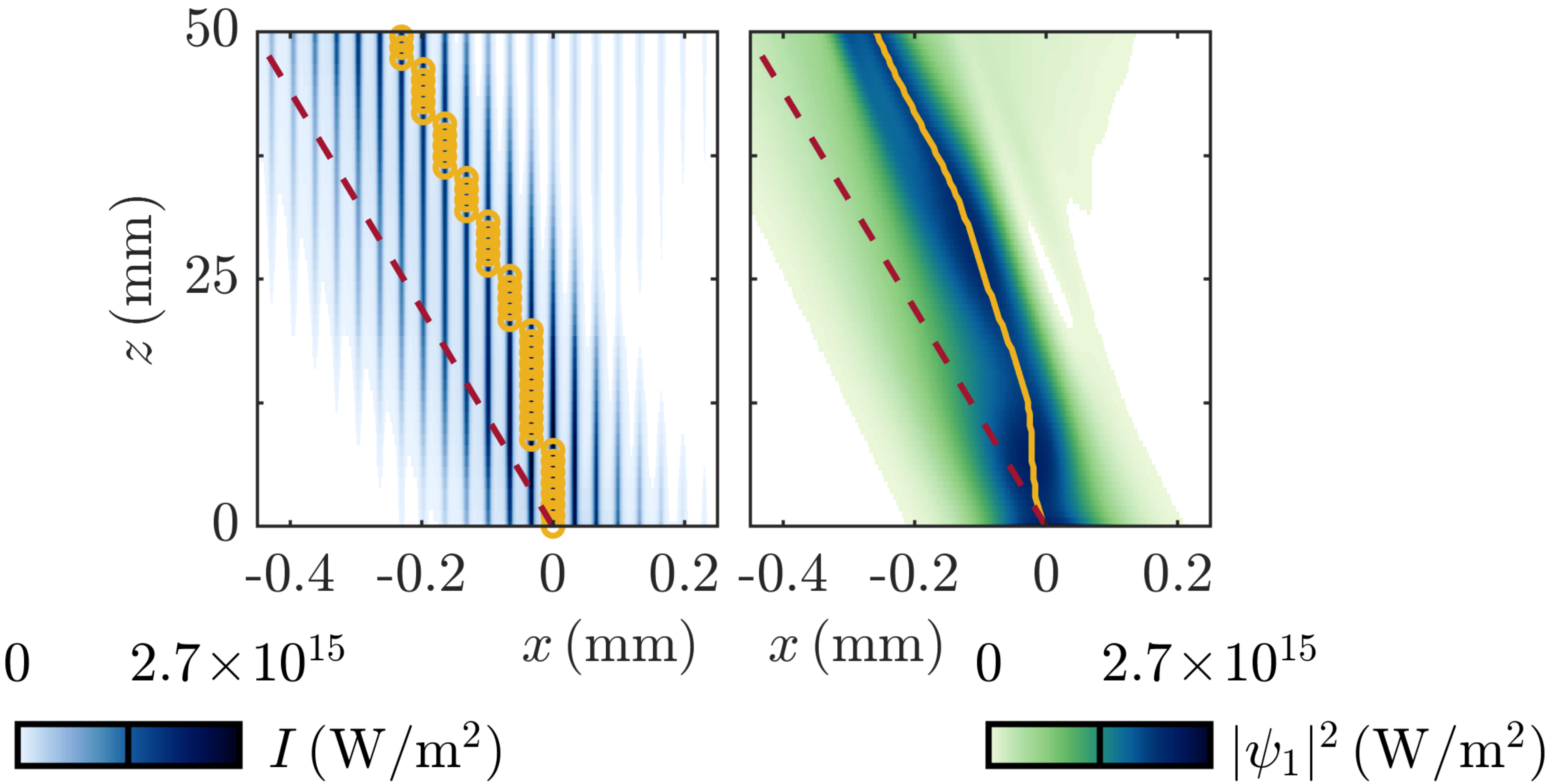

Modulational instability

- Breakup of uniform wave field under combined action of dispersion and nonlinearity
- Spontaneous formation of localized solitons and breathers

$$\frac{\partial A}{\partial z} + i\beta_2 \frac{\partial^2 A}{\partial t^2} = i\gamma |A|^2 A$$

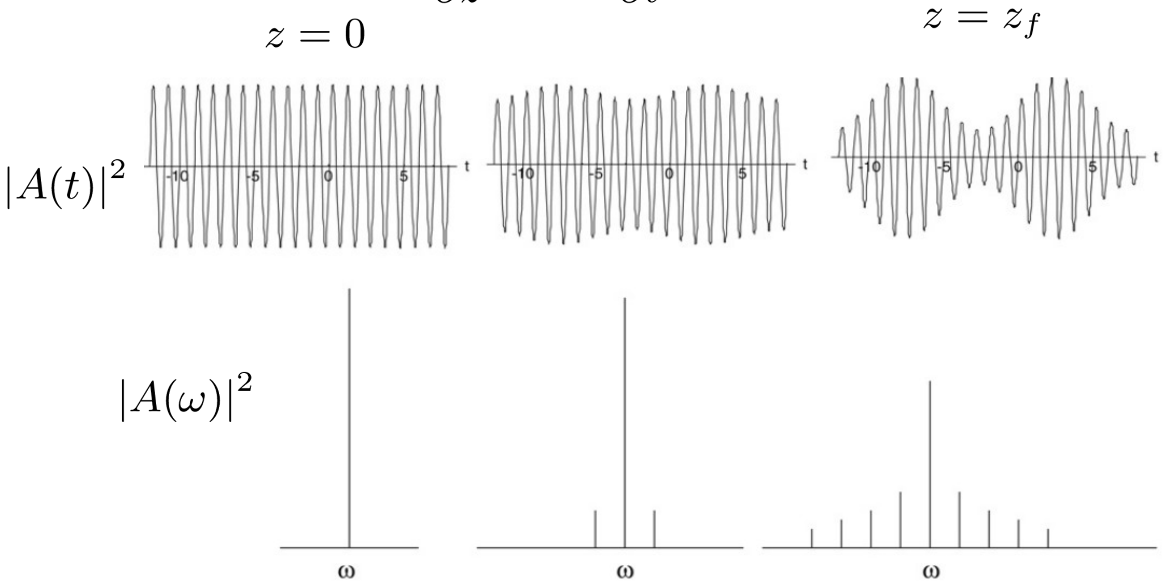

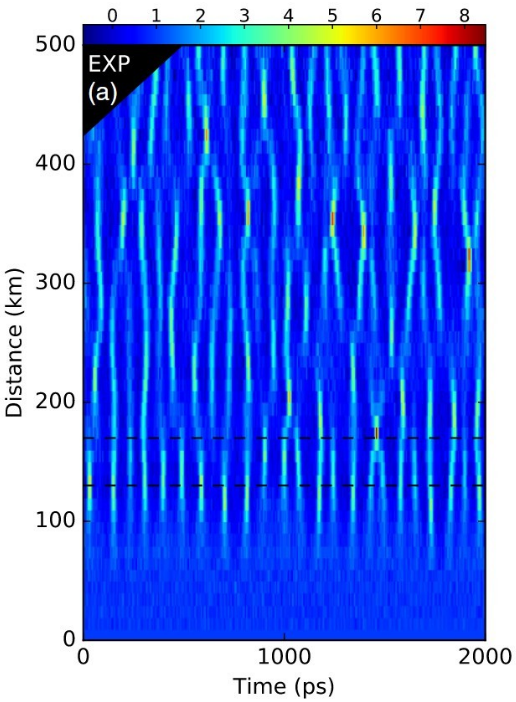

V. E. Zakharov, L. A. Ostrovsky, Physica D 238, **540** (2009)
A. E. Kraych et al., Phys. Rev. Lett. **123**, 093902 (2019)

What are the properties of modulational instability in topological photonic lattices?

Model: square lattice Chern insulator + Kerr nonlinearity

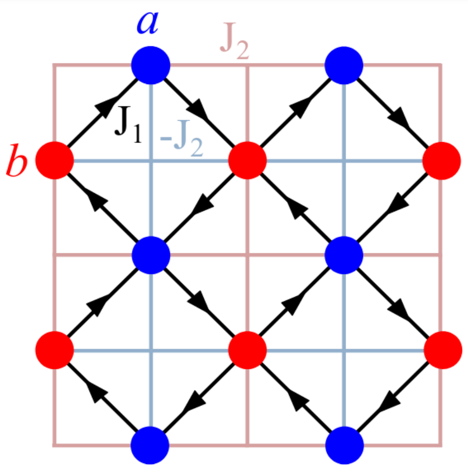

$$i\partial_t \psi_{\boldsymbol{r}} = \left(\hat{H}_L + \hat{H}_{NL}\right)\psi_{\boldsymbol{r}} \quad \hat{H}_{NL}\psi_{\boldsymbol{r}}^{(j)} = \Gamma f\left(\left|\psi_{\boldsymbol{r}}^{(j)}\right|^2\right)\psi_{\boldsymbol{r}}^{(j)}$$

$$\hat{H}_L(\mathbf{k}) = \boldsymbol{d}(\boldsymbol{k})\cdot\hat{\boldsymbol{\sigma}}, \quad d_z = \Delta + 2J_2\left(\cos k_x - \cos k_y\right)$$

$$d_x + id_y = J_1\left[e^{-i\pi/4}\left(1 + e^{i\left(k_y - k_x\right)}\right) + e^{i\pi/4}\left(e^{-ik_x} + e^{ik_y}\right)\right]$$

Bloch wave eigenstates $\hat{H}_L(\boldsymbol{k})u_n(\boldsymbol{k}) = E_n(\boldsymbol{k})u_n(\boldsymbol{k})$

Energy bands

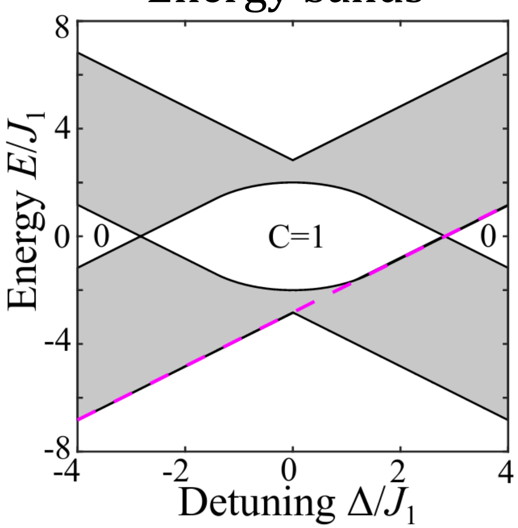

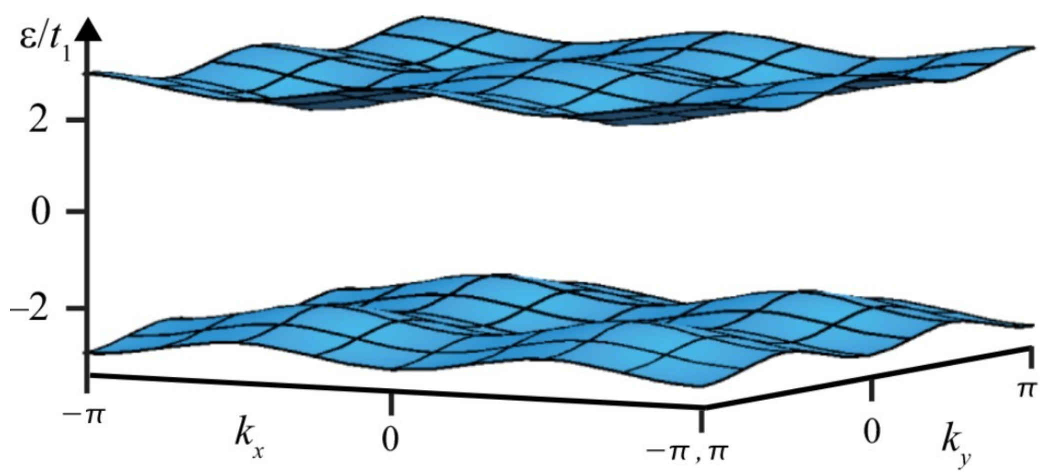

Neupert et al, Phys. Rev. Lett. **106**, 236804 (2011)

Linear stability analysis

Consider small perturbations to nonlinear Bloch wave $\psi_n(t) = (\phi_n + p_n(t))e^{-iEt}$

Compute linearised perturbation modes $p_n(t) = u_n e^{-i\lambda t} + v_n^* e^{-i\lambda^* t}$

Perturbation modes with positive $\mathrm{Im}\lambda$ are unstable

Stability re-emerges at nonlinearity-induced band crossing $\Delta + \Gamma I_0/2 = 4J_2$

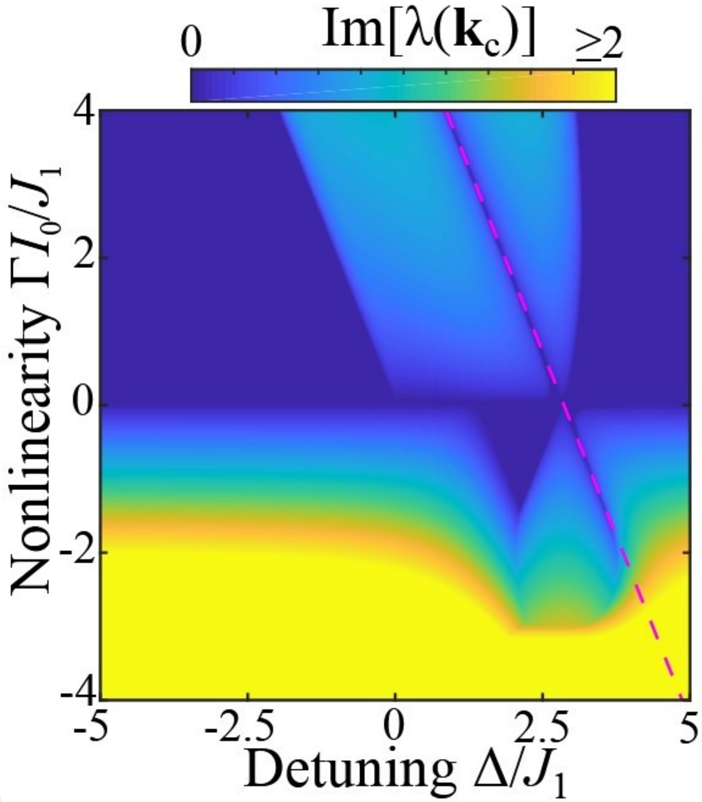

Bernevig–Hughes–Zhang Hamiltonian:

$$\hat{H}_L = -J_1\sqrt{2}\left(-p_x\hat{\sigma}_y + p_y\hat{\sigma}_x\right) +$$
$$+\left(\Delta - 4J_2 + J_2\left[p_x^2 + p_y^2\right]\right)\hat{\sigma}_z .$$

Nonlinear mode:

$$|\phi(r)\rangle = \left(\sqrt{I_0}, 0\right)^T e^{i\pi x}$$

$$E_{NL} = \Delta - 4J_2 + \Gamma f\left(I_0\right)$$

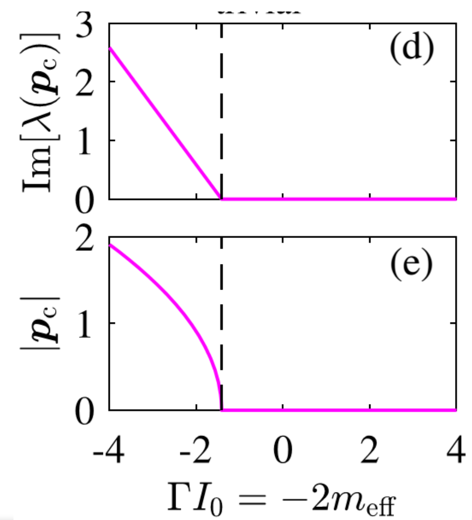

Nonlinear dynamics of Bloch waves

$$i\partial_t \psi_{\boldsymbol{r}} = \left(\hat{H}_L + \hat{H}_{NL}\right)\psi_{\boldsymbol{r}}$$

Real space participation number (fraction of strongly-excited lattice sites)

$$P_{\boldsymbol{r}} = \frac{\mathcal{P}^2}{2N^2}\sum_{\boldsymbol{r}}\left(\left|\psi_{\boldsymbol{r}}^{(a)}\right|^4 + \left|\psi_{\boldsymbol{r}}^{(b)}\right|^4\right)^{-1}$$

Fourier space participation number (fraction of strongly-excited Fourier modes)

$$P_{\boldsymbol{k}} = \frac{\mathcal{P}^2}{2N^2}\sum_{\boldsymbol{k}}\left(\left|\psi_{\boldsymbol{k}}^{(a)}\right|^4 + \left|\psi_{\boldsymbol{k}}^{(b)}\right|^4\right)^{-1}$$

Three instability regimes, depending on Γ and Δ

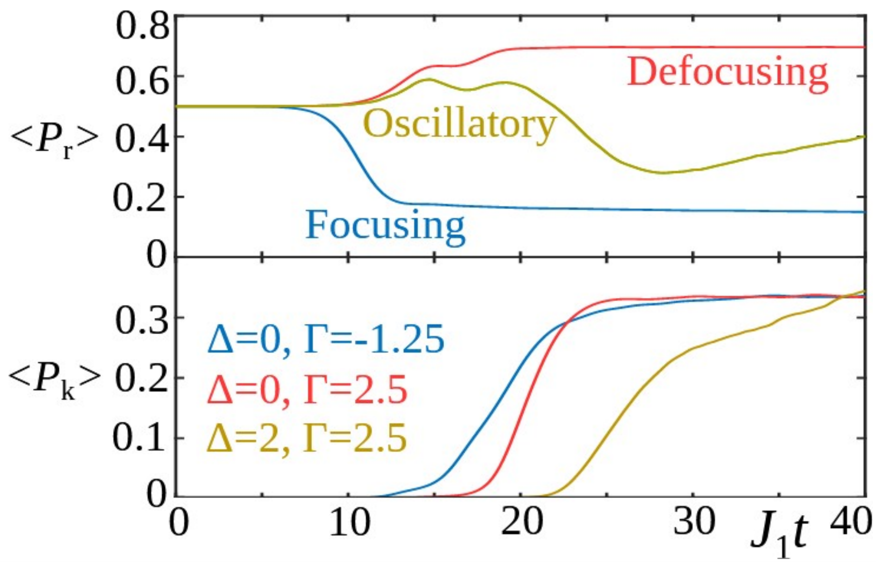

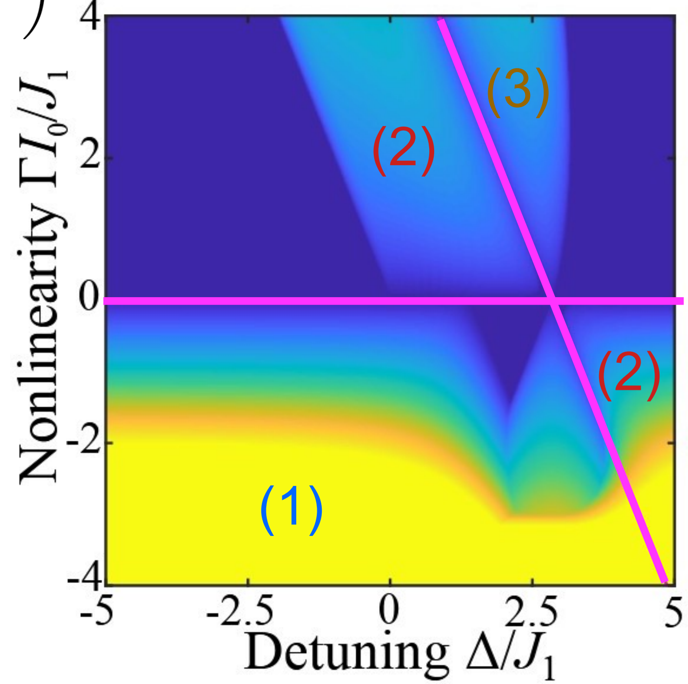

Self-focusing instability dynamics

Occurs when effective interactions are **attractive** $\Gamma m_{\mathrm{eff}} < 0$

Formation of localized solitons in the topological band gap

Spreading in Fourier space, exciting the entire Brillouin zone

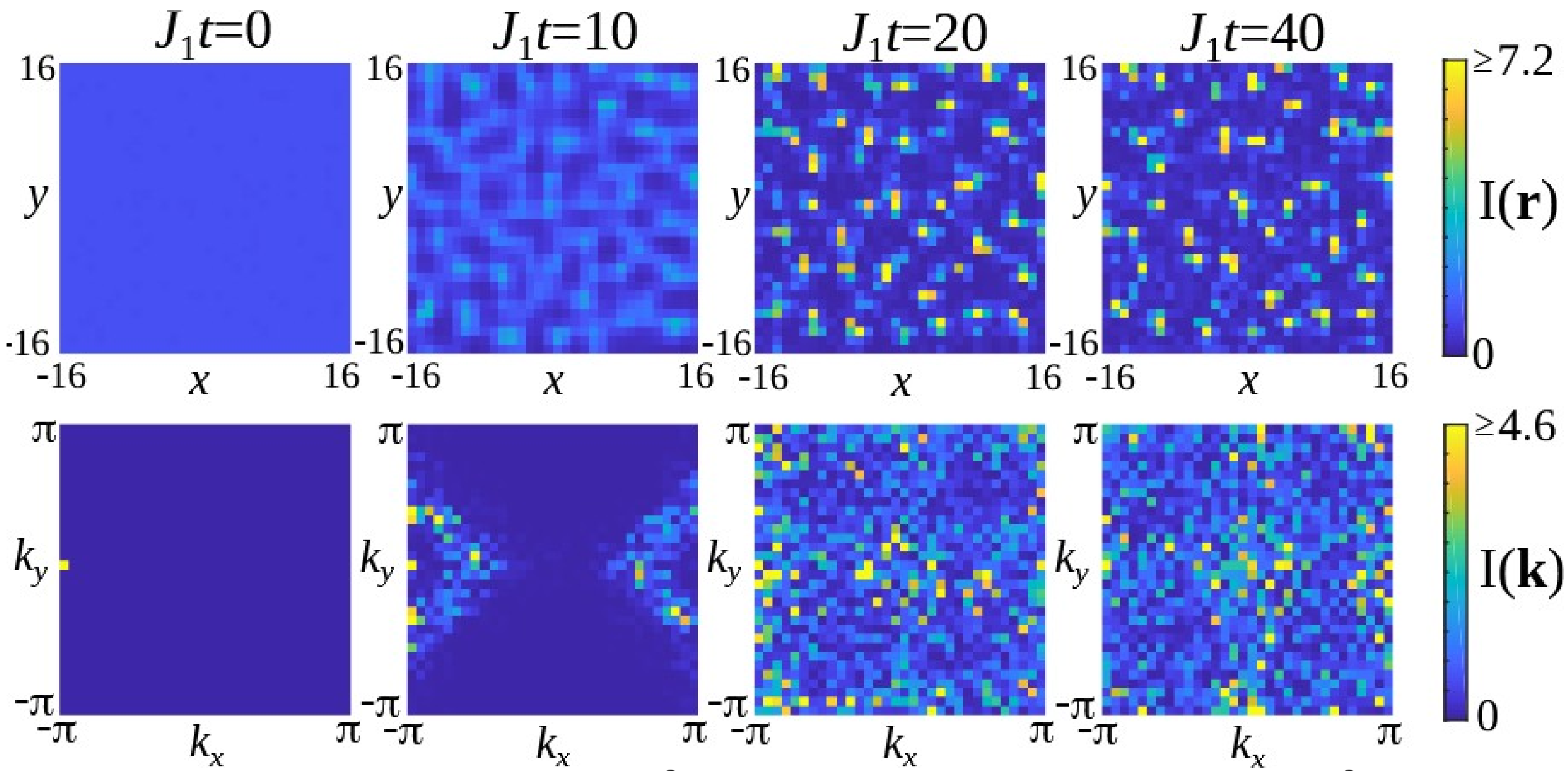

$I(\boldsymbol{r}) = |\psi_a(\boldsymbol{r})|^2 + |\psi_b(\boldsymbol{r})|^2$ $\quad$ $I(\boldsymbol{k}) = |\psi_a(\boldsymbol{k})|^2 + |\psi_b(\boldsymbol{k})|^2$

Self-defocusing instability dynamics

Occurs when effective interactions are **repulsive** $\Gamma m_{\text{eff}} > 0$

More uniform intensity in real space

Spreading in Fourier space, exciting the entire Brillouin zone

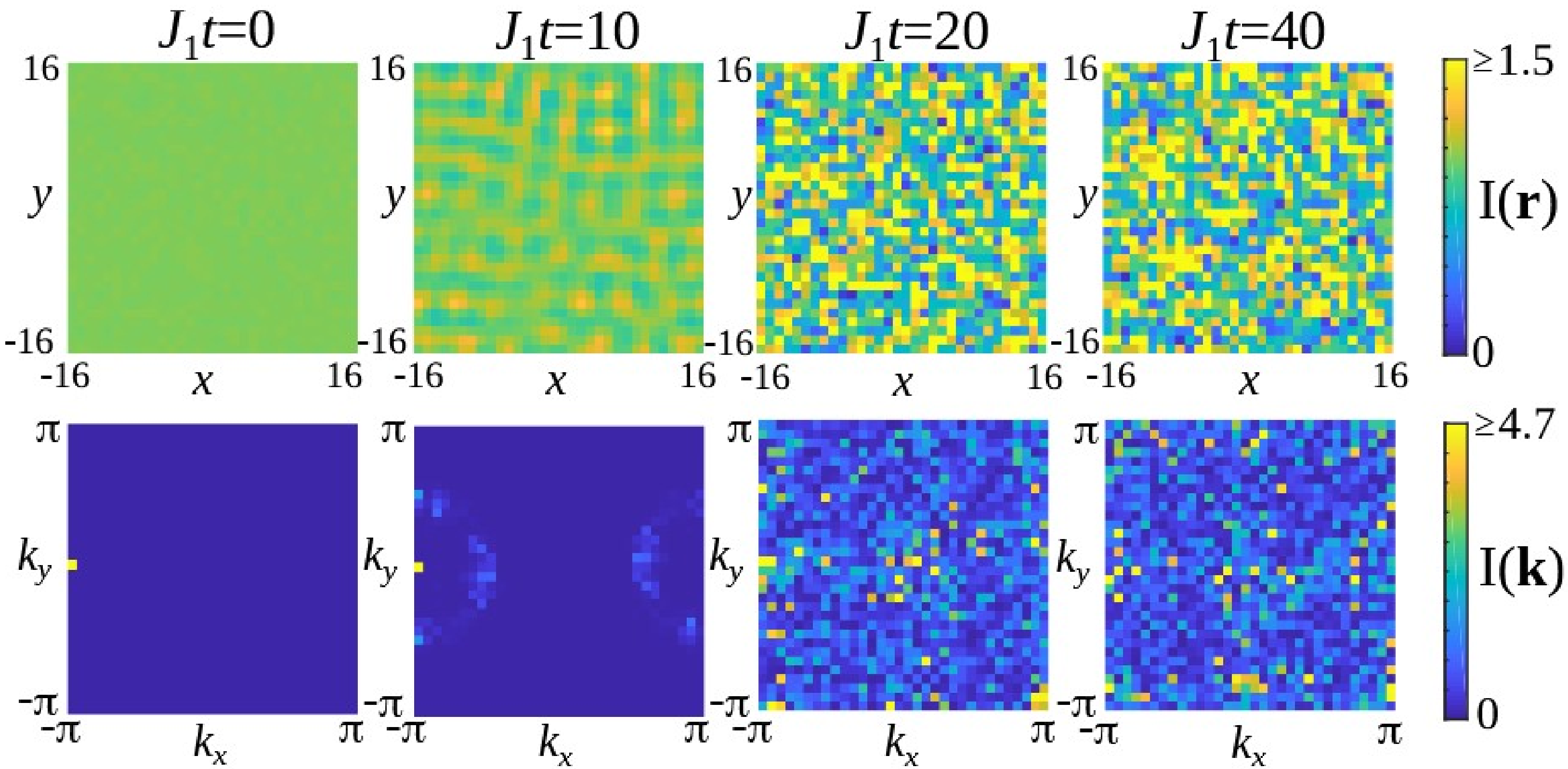

$I(\boldsymbol{r}) = |\psi_a(\boldsymbol{r})|^2 + |\psi_b(\boldsymbol{r})|^2$ $\quad$ $I(\boldsymbol{k}) = |\psi_a(\boldsymbol{k})|^2 + |\psi_b(\boldsymbol{k})|^2$

Oscillatory instability dynamics

Occurs when there is nonlinearity-induced band inversion $\Gamma I_0/2 > m_{\mathrm{eff}}$

No long-time steady state in real space

Spreading in Fourier space, exciting the entire Brillouin zone

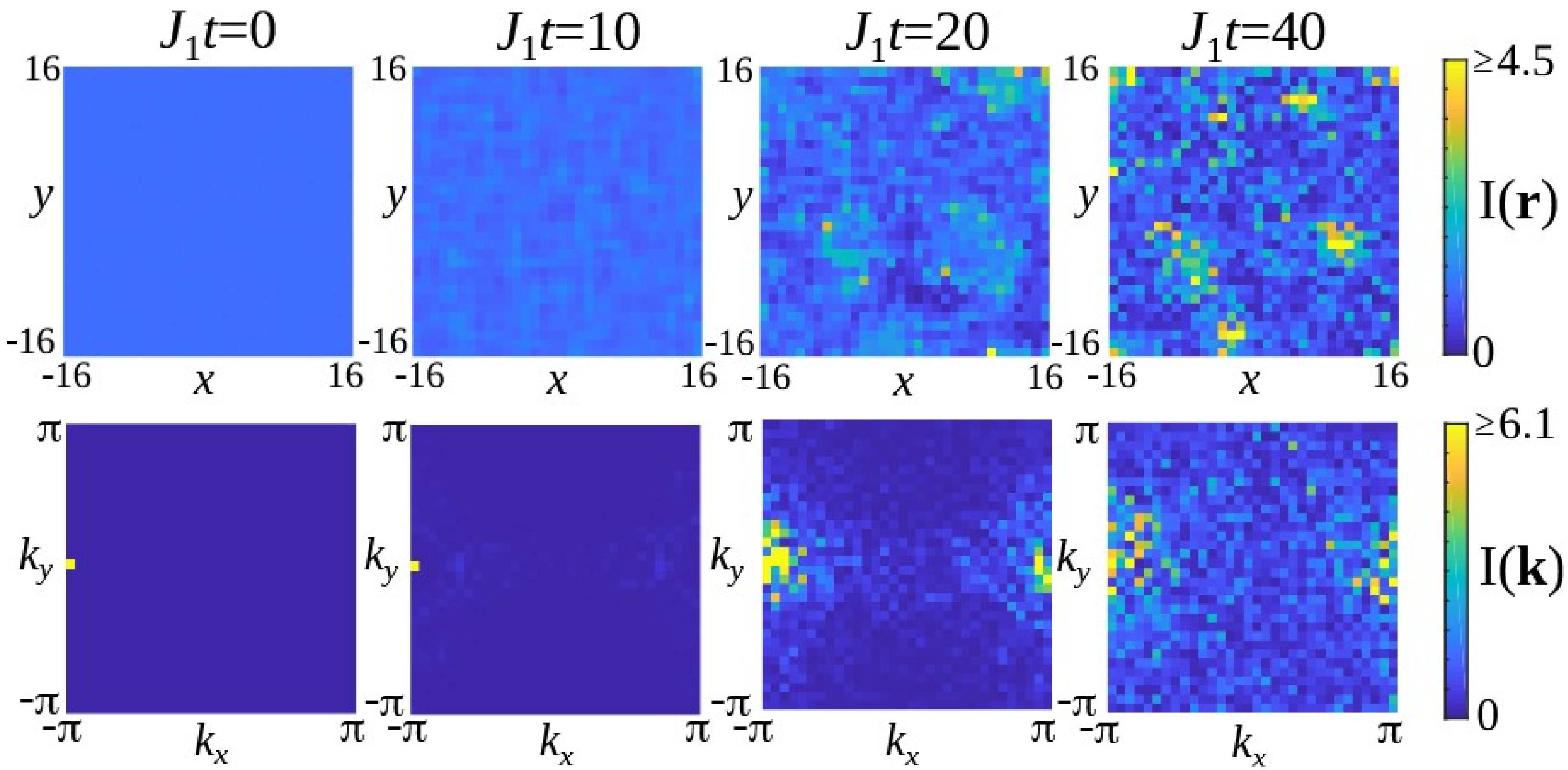

$I(\boldsymbol{r}) = |\psi_a(\boldsymbol{r})|^2 + |\,\psi_b(\boldsymbol{r})|^2$ $\quad I(\boldsymbol{k}) = |\psi_a(\boldsymbol{k})|^2 + |\,\psi_b(\boldsymbol{k})|^2$

Nonlinearity-induced mode mixing

Nonlinearity can induce intra-band or inter-band mixing

Oscillatory instability regime: strong persistent inter-band mixing

Focusing & defocusing regimes: field spreads within the initially-excited lower band

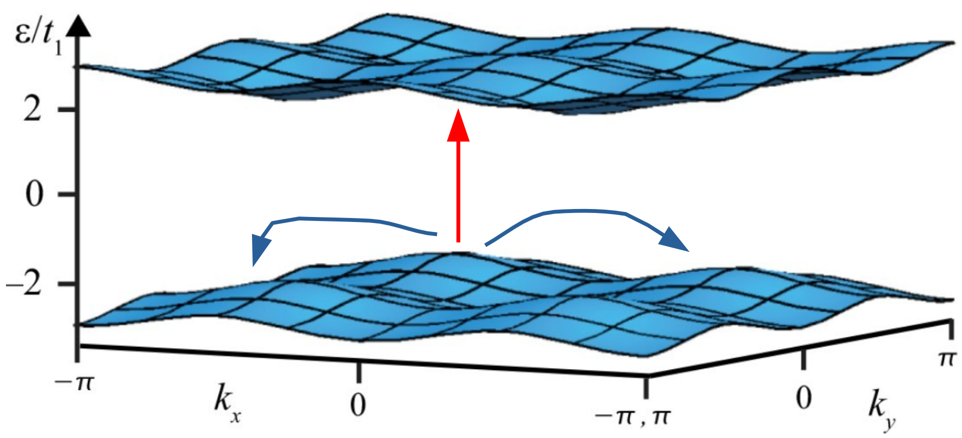

Upper band population

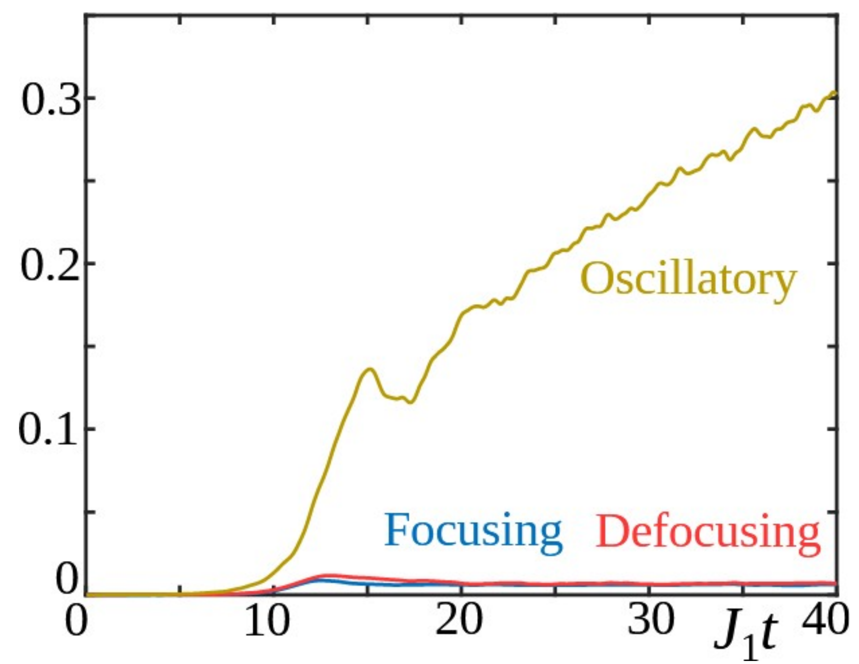

Probing Chern number

"Polarization" = field distribution between the two sublattices

Consider the field polarization averaged over initial perturbations $\langle \boldsymbol{n}(\boldsymbol{k}) \rangle$

Nonzero purity gap $\min_{\boldsymbol{k}}[\langle \boldsymbol{n}(\boldsymbol{k}) \rangle]$ when interband mixing strength is small,

field generated by instability has well-defined polarization

Bulk Chern number can be measured in focusing, defocusing instability regimes!

Fösel et al, New J. Phys. **19**, 115013 (2017)

Hu, Zoller, Budich, Phys. Rev. Lett. **117**, 126803 (2016)

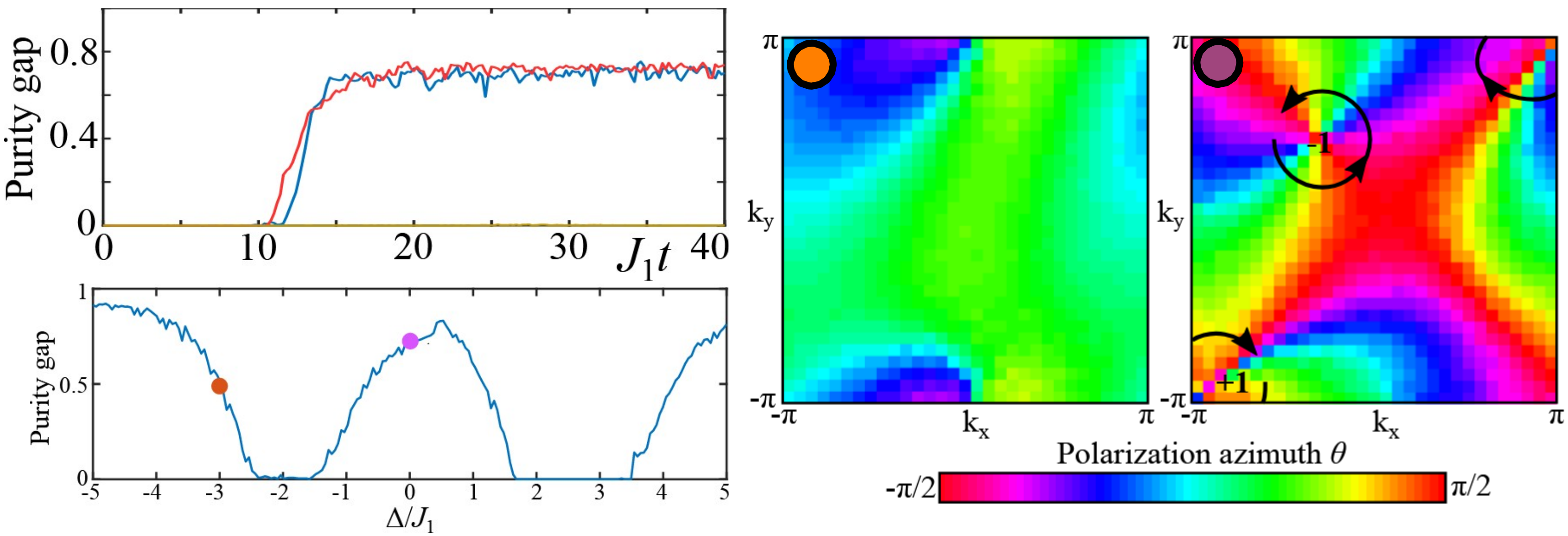

Summary on nonlinear waves in topological lattices

- ❑ Nonlinear Dirac model: topological gap solitons and nonlinear edge states
- ❑ Nonlinear tunability and nonlinear coupling to topological modes

Laser & Photon. Rev. **13**,1900223 (2019); Phys. Rev. A **98**, 013827 (2018); Light: Sci. Appl. **9**, 147 (2020)

- ❑ Edge wavepackets exhibit gradient catastrophe due to novel higher-order effective nonlinearities emerging for topological edge states

Phys. Rev. Research **3**, 043027 (2021)

- ❑ Bulk modulational instability in topological bands: different regimes sensitive to nonlinearity strength and topological band inversions

Phys. Rev. Lett. **126**, 073901 (2021)

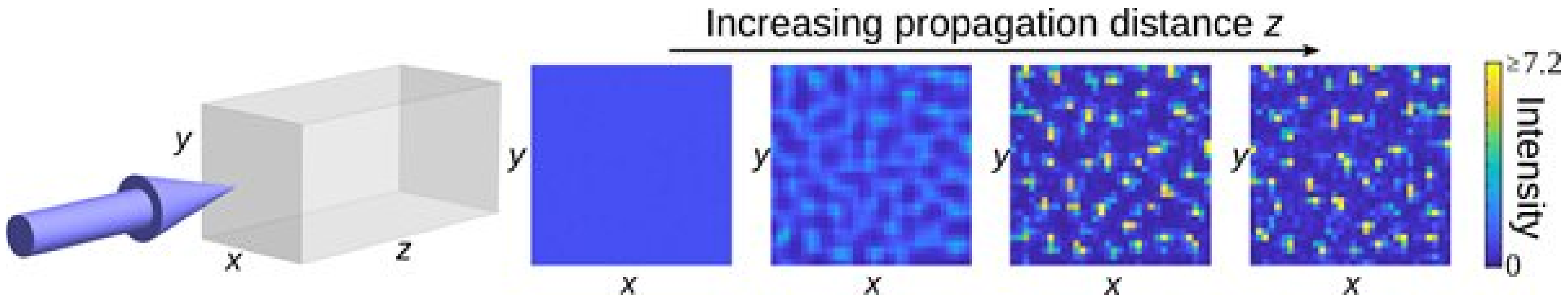

Email: daria.smirnova@anu.edu.au